universität wien

MASTERARBEIT

Titel der Masterarbeit

„Structural features of the MAP1b light chain 1 microtubule binding domain“

verfasst von

Markus Huber BSc

angestrebter akademischer Grad

Master of Science (MSc)

Wien, 2015

Studienkennzahl lt. Studienblatt:	A 066 834
Studienrichtung lt. Studienblatt:	Master Molekulare Biologie
Betreut von:	ao. Univ.-Prof. Dr. Friedrich Propst

Acknowledgements

I want to thank my supervisor Friedrich Propst for providing me the opportunity to do my Masters thesis in his lab at the MFPL in Vienna. I greatly welcomed our discussions about the project but also our various conversations about society and politics.

I also thank Robert Konrat for all his ideas and suggestions on how to proceed with our NMR measurements. At this point I also want to mention Thomas Schwarz who did most of the NMR spectroscopy and helped me to understand the underlying theories. Thank you.

I thank Zsuzsanna Orban-Nemeth who thought me much about FPLC and protein purification in general. I also want to thank Irmgard Fischer for all her help with the tubulin preparation and various other things.

At last, I thank all my colleagues from the Propst, Fuchs and Wiche groups. They had always time for me when I needed help and made events and activities outside the lab a lot more fun.

Abstract

Microtubule associated proteins (MAPs) constitute a superfamily of microtubule binding proteins that are involved in the regulation of microtubules. MAPs interact with tubulin subunits or microtubules and mostly stabilize the microtubule structure or enhance microtubule polymerisation. Classical MAPs include 4 families: MAP1, MAP2, tau and MAP4. While the later three show a common microtubule interaction motif that involves a set of homologous repeats, Map1 proteins lack this mutuality and interact with microtubules in a different way. This makes the MAP1 family particularly interesting. MAP1a, MAP1b and MAP1s (the 3 family members) are all translated as precursors and cleaved proteolytically into a heavy and a light chain. MAP1b, consisting of the MAP1b heavy chain and light chain 1 (LC1), is the best characterised family member. It is highly expressed in neurons and is essential for neuronal network formation during brain development. It is involved in axon guidance and neural polarization and is necessary for the formation of the corpus callosum. Deregulation may lead to ataxia, fragile x mental retardation or giant axonal neuropathy. Although both, the MAP1b heavy chain and LC1, contain microtubule binding domains, LC1 was found to be the main microtubule binding unit. Our goal was to look at the LC1 microtubule binding domain to determine the structure and identify amino acids responsible for the interaction with microtubules. Therefore we introduced 4 missense mutations in the wild-type LC1 microtubule binding domain and tagged them with a paramagnetic spin label (MTSL). The wild-type and MTSL-tagged mutant proteins were measured with ^{1}H-^{15}N-HSQC in the presence of microtubules or tubulin. Our results suggest that there are 3 areas with different affinity for microtubules. Moreover, our data indicates that interaction with microtubules is contingent on the formation of an α-helix at the NH_2 terminus of LC1.

Zusammenfassung

Mikrotubuli assozierte Proteine (MAPs) bilden eine Superfamilie aus Microtubuli-bindenden Proteinen die an der Regulierung von Microtubuli beteiligt sind. MAPs interagieren mit Tubulin-Untereinheiten oder Mikrotubuli und stabilisieren häufig die Struktur von Mikrotubuli oder fördern deren Polymerisierung. Klassische MAPs umfassen 4 Familien: MAP1, MAP2, tau und MAP4. Während die letzen drei ein gemeinsames Microtubuliinteraktionsmotiv aufweisen, das eine Reihe von homologen "repeatsëinschließt, fehlt diese Gemeinsamkeit in den MAP1 Proteinen, die auf andere Weise mit Mikrotubuli interagieren. Das macht die MAP1-Familie besonders interessant. MAP1a, MAP1b und MAP1s (die 3 Familienmitglieder) werden alle 3 als Vorstufe translatiert und danach proteolytisch in eine schwere und eine leichte Kette gespalten. MAP1b, bestehend aus der MAP1b schweren Kette und der leichten Kette 1 (LC1), ist das am besten beschriebene Familienmitglied. Es zeigt eine hohe Expression in Neuronen und ist für die Errichtung des neuronalen Netzwerks während der Entwicklung des Gehirns erforderlich. Es ist an der Wegfindung der Axone und an der Polarisierung der Neuronen beteiligt und ist für die Entstehung des Gehirnbalken notwendig. Deregulierung kann zu Ataxie, dem Fragiles-X-assoziertes Tremor-Syndrom, oder zur Giant Axon Neuropathie führen. Obwohl beide, die MAP1b schwere Kette und die LC1, Microtubulebindedomänen enthalten, wurde festgestellt das LC1 vornehmlich den Mikrotubuli-bindenden Teil darstellt. Unser Ziel war die Analyse der LC1-Mikrotubulibindedomäne um dessen Struktur zu bestimmen und herauszufinden welche Aminosäuren für die Interaktion mit Microtubuli berantwortlich sind. Dazu wurden 4 „Missense“-Mutationen in den Wildtyp der LC1 eingebaut und diese mit einem paramagnetischen „spin label“ (MTSL) markiert. Die Wildtyp- und MTSL-markierten Proteine wurden mit ^{1}H-^{15}N-HSQC in Gegenwart von Microtubuli oder Tubulin gemessen. Unsere Ergebnisse zeigen dass 3 unterschiedliche Bereiche mit abweichender Affinität für Mikrotubuli existieren. Zudem deuten unsere Daten darauf hin, dass eine Interaktion mit Mikrotubuli von der Ausbildung einer α-Helix am NH_2-Terminus von LC1 abhängig ist.

Contents

List of Figures

List of Tables

1 Introduction

1.1 Microtubules

Microtubules are one of the major parts of the cytoskeleton in eukaryotic cells. Along with other components like actin and intermediate filaments they form a meshwork spanning the cell, thereby maintaining the cellular structure and providing routes for intracellular transport. One of the fundamental features of microtubules is their dynamic behaviour, allowing them to adapt very rapidly to changes in and around cells. [1–3]

1.1.1 Microtubule structure

Microtubules are built by small subunits called tubulins. The two most common of the family are α- and β-tubulin with about 55 kDa each. Proper folding of the two subunits depends on binding to a chaperon, the TCP-1 complex. After their release they arrange themselves to form polar α-β-heterodimers. One GTP (guanosine triphosphate) is stably bound to α-tubulin. A second GTP is attached transiently to the β-subunit and may get hydrolysed and exchanged. By aligning head to tail, tubulin heterodimers are able to form elongated protofilaments with the β-tubulin pointing towards the so called plus end. A second interaction between neighbouring tubulin molecules leads to parallel bundles of those protofilaments (see 1). Bundling is based on lateral contacts mainly between tubulin-subunits of the same type (α-α and β-β) and leads usually to hollow cylindrical microtubules consisting of 13 protofilaments with an outer diameter of about 24 nm. The protofilaments bundled to each other are shifted longitudinal in relation to the neighbouring filaments, leading to a helical lattice of heterodimers. This lattice contains a discontinuity after each turn (also called seam) were lateral contacts are made between α- and β-tubulins (instead of α-α and β-β). [1–4]

1.1.2 Microtubule dynamics

Microtubules are polar (due to their polar subunits) with a so called minus end, generally anchored at an organization centre (centrosome), and a plus end at the growing tip. The centrosome contains a third family member: γ-tubulin. This organization centre plays an important role in microtubule nucleation throughout the cell cycle and is often required to start

the process of microtubule formation. While the minus end is generally anchored and stable, the tip undergoes rapid changes leading to periods of polymerization and depolymerization. GTP bound to the β-subunit is largely involved in this dynamic instability. While GTP is bound to β-tubulin at the growing end of microtubules (a GTP-cap is protecting the tip), growth is favoured. However, each GTP may get hydrolysed as soon as another heterodimer is incorporated. This is caused by contacts between α-tubulin of newly bound heterodimers and β-tubulins of the former tip and happens for each protofilament separately. Moreover, the fate of a microtubule depends on its protofilaments. As long as new heterodimers are added faster than hydrolysis can take place in a majority of protofilaments, the microtubule plus end keeps a GTP-cap and grows further. If the heterodimers get scarce or something else delays the incorporation of new subunits, hydrolysis will become faster than polymerization and thus the GTP-cap will be lost. When this so called catastrophe happens, the microtubule starts to shrink rapidly. The GDP-heterodimers are pealed of the microtubule and recycled by exchanging their GDP with GTP, thus they are able to promote microtubule growth again. As soon as GTP-heterodimers are incorporated fast enough, the microtubule may be rescued from depolymerization and growth can start again. [1–4]

There are various substances that can interfere with polymerization or depolymerization of microtubules. One of them is taxol, a drug that is also used for cancer treatment. It stabilizes microtubules and prevents their depolymerization. This leads to cell cycle arrest and hence stops cell proliferation. Taxol is also used for in vitro experiments, if stable microtubules for certain measurements are required. [5]

1.1.3 Microtubule function

Microtubules are involved in an immense amount of functions throughout the lifetime of a cell. They build a network of traffic lanes for intracellular transport of molecules and play an important role in cell migration (axon growth) and polarization. Furthermore, they form the spindle apparatus in mitosis and meiosis, separating chromosomes and sister chromatids. All these processes are dependent on microtubules and their dynamic behaviour. However, there are a number of proteins collaborating with microtubules by adjusting them, or providing a distinct function themselves. [1, 3, 4]

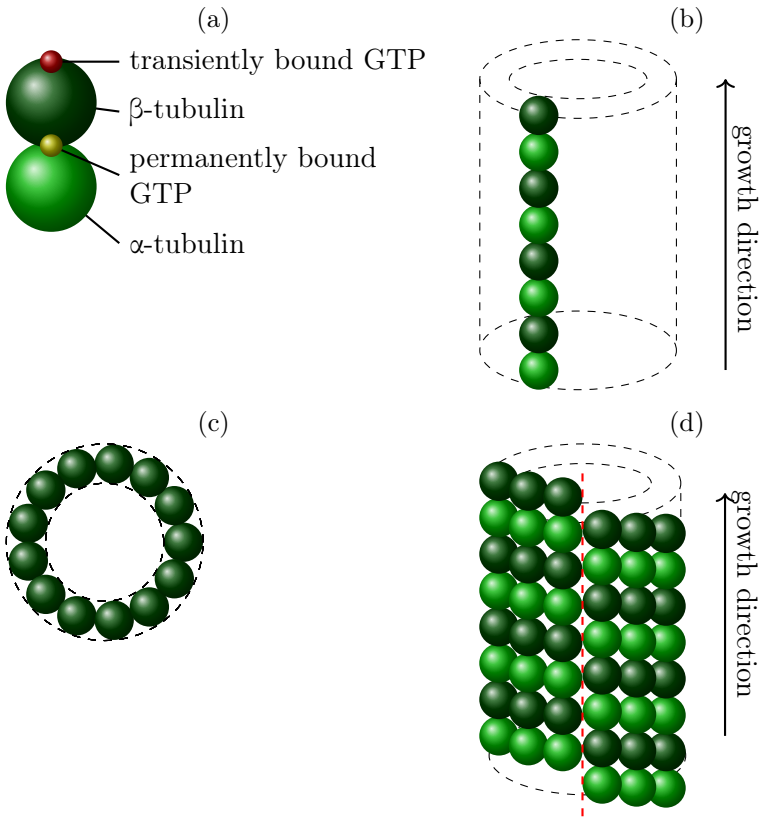

Figure 1: Microtubule structure - The tubulin heterodimer (a) is built by α- (light green) and β-subunits (dark green). GTP is bound permanently to the α-subunit (yellow). A second GTP is bound to the β-subunit but can be hydrolysed and exchanged (red). The dimers align head to tail to form protofilaments (b) and side by side to form sheet like structures. 13 subunits are oriented in a helical fashion and build a hollow cylindrical structure (c-d) with a discontinuity (also called seam) in the helical lattice (red).

1.2 Microtubule binding proteins

1.2.1 Motor proteins

Cytoskeletal motor proteins like kinesins and dyneins transport cargo along microtubules. While dyneins are a group of minus end directed motor proteins, most kinesins move to the plus end. Some kinesins are however helping in the minus end directed transport or function as catastrophe factors on microtubules, promoting depolymerisation. Movement of both microtubule motors depends on ATP, which is hydrolysed in order to generate mechanical force. [6–8]

Dyneins and kinesins were shown to share an overlapping binding site on microtubules at the β-subunits COOH-terminal region around residues 403 to 430 [9–11]. Interaction of kinesins with microtubules seems to rely on a cluster of 3 loops in its motor domain. Binding may occur mainly by ionic interactions of amino acids in this regions [12]. Dynein binding to microtubules was shown to depend on a small globular domain at the end of an anti-parallel coiled-coiled stalk emerging from its motor domain [13].

1.2.2 Plus-end-tracking proteins

Another group of microtubule binding proteins are plus-end-tracking proteins (+TIPs). They accumulate at the plus ends of microtubules, either by interacting directly with the microtubule tip, or by plus-end directed transport (either moving to the plus ends on their own, or by "hitchhiking" with other proteins). Most +TIPs modulate microtubule dynamics by reducing catastrophes or supporting rescues, thereby stabilizing them (for example CLIP-170, CLASP, dynein/dynactin, etc.). Moreover, some may function as anchor points, promoting capture of microtubule plus ends at intracellular structures like the plasma membrane. Interaction of +TIPs with microtubules greatly depends on the interaction between +TIPs themselves. Thus, absence of core +TIPs may prevent accumulation of other +TIPs. The end binding (EB) protein family was shown to be a core component and pioneer of +TIPs. EB proteins contain conserved, globular calponin homology (CH) domains at their NH_2 termius, that are both necessary and sufficient for microtubule binding. Interaction with microtubules appears to be due to the recognition of structural features on the plus ends that are characteristic for the GTP cap. [14, 15]

1.2.3 Heterodimer binding proteins

Microtubules are not only regulated at the level of polymerized filaments, but also via their subunits. The first protein found to be involved in this kind of regulation was stathmin, a cytosolic phosphoprotein. By interacting with heterodimers it regulates microtubules simply by withdrawing dimer-subunits from (respectively releasing them to) the pool of free tubulin-dimers in the cell. X-Ray crystalography of the stathmin like domain of RB3 (a stathmin family member) showed an elongated α-helical binding domain. This α-helix interacts with

two tubulin-dimers, aligned head to tail. Complex formation with the stathmin like domain involves either NH_2- or COOH-terminal regions on each of the α- and β-subunits. [16, 17]

1.2.4 Classical MAPs

Microtubule associated proteins (MAPs, or classical MAPs) are another superfamily of proteins involved in the dynamics and regulation of microtubules [18, 19]. The superfamily divides into the 4 families MAP1, MAP2, MAP4 and tau. The best known of those proteins are the MAP2 members and tau. Tau comes in 7 different isoforms, with the biggest of them only present in the peripheral nerves. Binding to microtubules is mediated by repeats of 18 amino acids. Tau not only stabilizes microtubules but also promotes growth and mediates the formation of parallel microtubule bundles. Defects in tau proteins are very commonly linked to Alzheimer's disease. MAP2 has similar effects on microtubules as tau and shares some homologous repeats contributing to microtubule binding, although microtubules seem to be further apart when bundled by MAP2 compared to tau. MAP4 shows resemblance with MAP2 and tau regarding the homologous repeats interacting with microtubules. However, while tau and MAP2-proteins are mainly expressed in neurons, MAP4 is expressed in many different cell types. In contrast to the majority of MAPs sharing a similar interaction model, MAP1 proteins are believed to bind to microtubules rather though their own, unique binding motifs. [1, 18–20]

However, until now there is no detailed binding model for the MAP1-family proteins making their investigation exceedingly interesting.

1.3 MAP1 family

1.3.1 Structure

The MAP1 family consists of 3 members, namely MAP1a, MAP1b and MAP1s. All three are protein complexes built from at least one heavy and one or more light chains. The chains are synthesised as parts of a polyprotein that is cleaved proteolytically after synthesis. This cleavage leads to the MAP1a heavy chain (350 kDa) and light chain 2 (LC2, 28 kDa in size), the MAP1b heavy chain (300 kDa) and light chain 1 (LC1, 32 kDa in size), and the MAP1s heavy chain (100 kDa) and its light chain (26 kDa). While the MAP1s light chain forms a

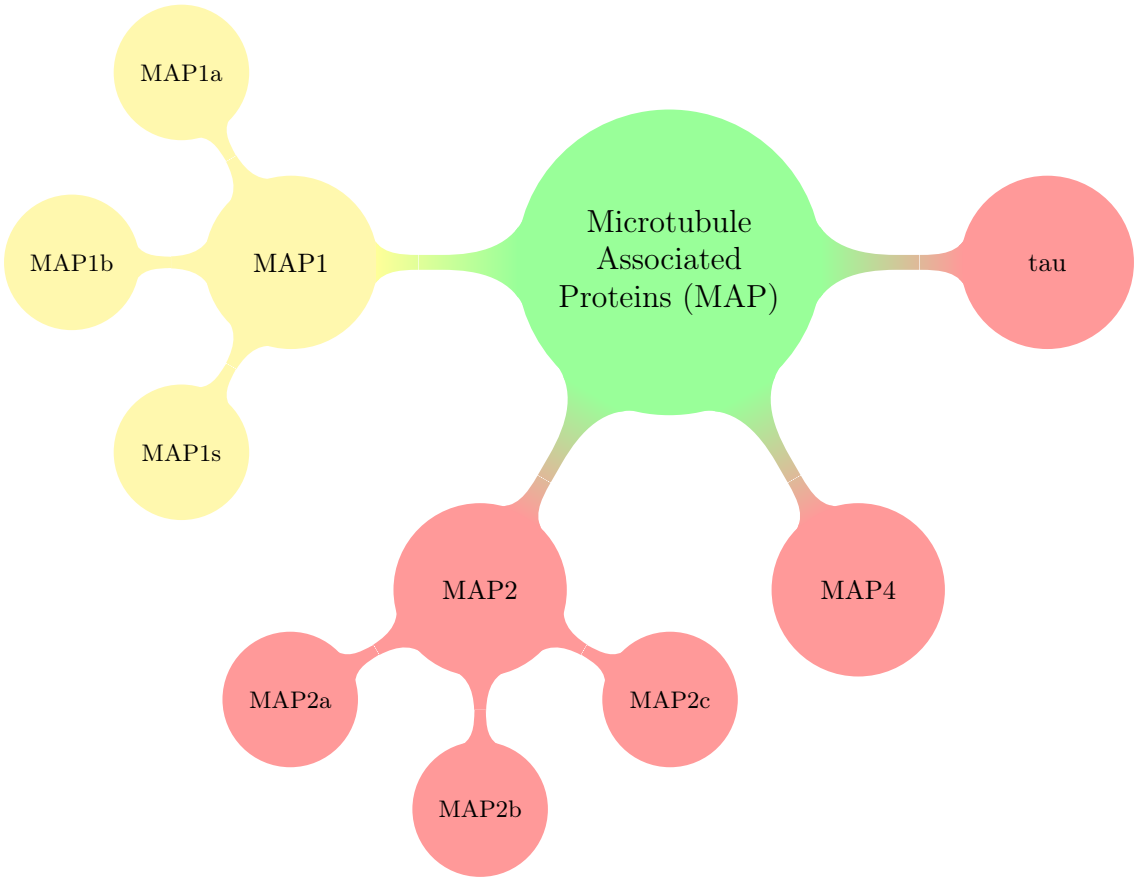

Figure 2: The superfamily of microtubule associated proteins - The superfamily consists of 4 families: MAP1, MAP2, tau and MAP4. While MAP2, MAP4 and tau share some resemblance in microtubule binding, the MAP1 family differs from them.

complex solely with the MAP1s heavy chain, LC1 and LC2 are exchangeable and can both bind to MAP1a and MAP1b [19, 21, 22]. Furthermore, a third light chain (light chain 3, with 18 kDa in size) is able to bind to MAP1a and MAP1b. It is the product of a separate gene, there is no sequence similarity to the other chains and it is usually not considered to be part of the MAP1 protein family [18, 23].

Although the relevance is not clear, alternative splicing in MAP1b has been reported [24].

There are 3 homology domains on the NH_2 and COOH termini of the heavy chains and the COOH terminus of the light chains (see figure 3) [19, 21]. The last one (MH3) is able to bind actin in its filamentous form (F-actin) and to the NH_2-terminal domain of the heavy chain (MH1) [19, 25]. The sequence of the light chain's NH_2 terminus is not conserved in the 3 family members, but in each light chain it is capable to bind microtubules [19, 25]. The light chain

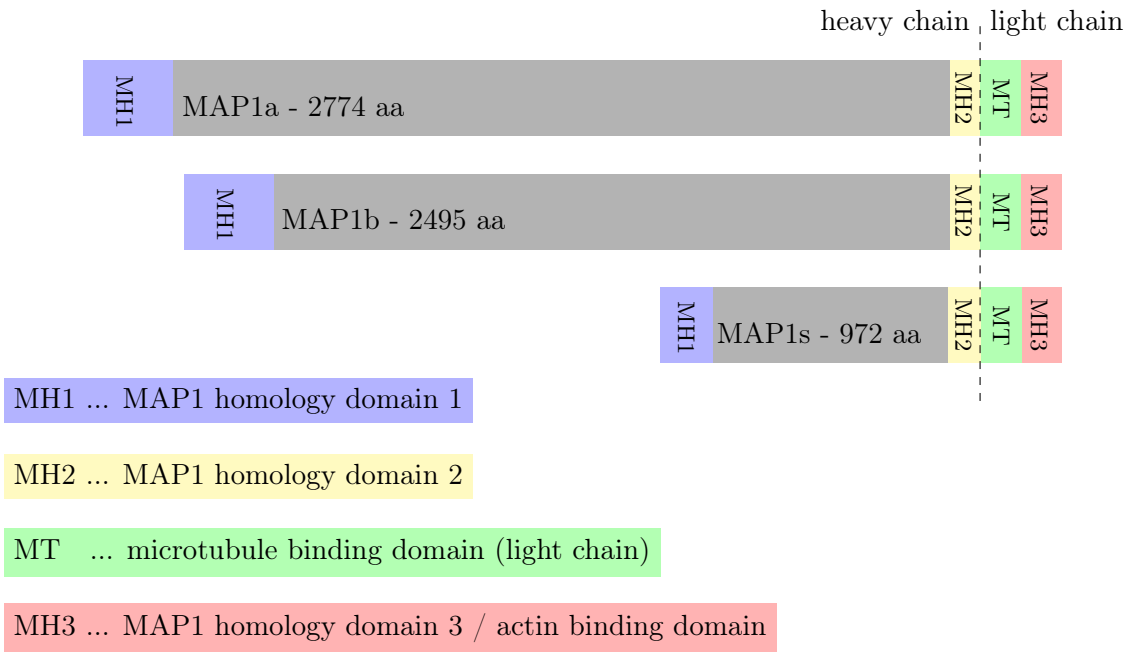

Figure 3: Domain structure of MAP1 proteins - The MAP1 family members are translated as precursors and cleaved into heavy and light chains. The family contains 3 conserved domains: MH1, MH2 and MH3. MH3 allows binding to F-actin and along with MH1 enables interaction of light and heavy chains. While LC1 and LC2 (originating from the MAP1b respectively MAP1a precursors) may both bind to MAP1a and MAP1b heavy chains, the MAP1s light chain is limited to its own heavy chain.

1 microtubule binding domain (LC1-MTB) lacks an ordered 3-dimensional structure which is referred to as intrinsically disordered. In addition to the light chains, both MAP1a and MAP1b heavy chains contain microtubule binding sites [26, 27].

1.3.2 Distribution

The MAP1 family members MAP1a and MAP1b are expressed mainly in the nervous system. MAP1a is preferentially localized to dendrites in adult neurons. It plays an important role as adaptor protein in postsynaptic densities, where defects are linked to hearing loss. MAP1b on the other hand is mainly distributed to axons, especially in growing ones. It stabilizes microtubules similar to tau (although less strong) and leads to wavy instead of straight microtubule bundles when overexpressed. MAP1s is more widely distributed than the other two family members with the highest expression levels in testis and brain. [18, 19]

1.4 MAP1b

1.4.1 Function

The best characterised protein of the MAP1 family is MAP1b. It stabilizes microtubules and may play a role in the coupling of microtubule and actin movement [28]. The stabilizing effects on microtubules [29] are regulated by phosphorylation through glycogen synthase kinase-3 β (GSK3β). Two residues, serine 1260 and threonine 1265, are targeted by GSK3β and phosphorylated especially in growing axons [30, 31]. During complex formation the MAP1b heavy chain was found to suppress binding of LC1 to microtubules [32]. Additionally, regulation of LC1 binding to microtubules is subject to auto inhibition probably occurring through an intramolecular interaction of its COOH and NH_2 terminus. This interaction can be inhibited by S-nitrosylation at cysteine 2457 in response to an increase in intracellular Ca^{2+} concentration leading to enhanced microtubule binding [33].

MAP1b is highly expressed during regeneration and development of neurons [34]. It is essential for neuronal network formation during brain development and formation of synapses in mice. Moreover, MAP1b shows involvement in axon guidance and neural polarization [35–38]. Removal of MAP1b results in a failure to form prominent brain cummissures such as the corpus callosum and leads to other disruptions of the neuronal network [36, 38]. Overexpression or deregulation has been linked mainly to 3 neuronal diseases [39–43]:

Giant axonal neuropathy

A disorganization of neurofilaments leading to giant axons, disturbing proper signal transmission.

Fragile X mental retardation

A mutation on the X chromosome leading to autism and mental disability.

Ataxia

A dysfunction of parts of the nervous system responsible for movement.

1.4.2 Structure

Structural details of the MAP1b heavy/light chain complex are still largely unknown. Electron microscopy shows a rod-shaped overall structure with a globular terminal domain on the tip [6]. Furthermore, structure predictions of the MAP1b homologue Futsch in *Drosophila melanogaster* suggest an unfolded structure spanning at least 50 % of the protein [18].

1.5 NMR

Nuclear magnetic resonance (NMR) occurs when atomic nuclei with a certain spin are affected by a magnetic field and probed by a distinct frequency. A spin is a fundamental property of each proton, neutron and electron, although only protons and neutrons influence the nuclear spin. Since spins of opposite signs cancel each other out, only atoms with unpaired protons or neutrons (hence atoms with odd mass or atomic numbers) have a spin other than 0 and can be affected by a magnetic field. Additionally, only nuclei with a dipole-moment (either the mass or the atomic number has to be odd, but not both) are suitable for NMR. Signals from nuclei with a quadrupole-moment (for example ^{14}N with 7 neutrons and protons) are very hard to detect and thus are not applicable. The applied magnetic field forces particles with nuclear spins to align either with (low energy state) or opposite the field. In general a slightly higher number of spins align with the field than against it. However, by absorbing the right amount of energy a transition to align the particle opposite the field (high energy state) is possible. The same is correct for a transition in the other direction, thereby emitting energy that can be measured. The energy amount depends on the resonance frequency (also Larmor frequency) of the particle and the magnetic field (see figure 4).

Because the resonance frequency of a nucleus depends on the strength of the magnetic field applied to it, comparison of spectra gained at different field strengths would be difficult. Therefore the term chemical shift was introduced. The chemical shift is the resonance frequency of a nucleus relative to a standard, generally Tetramethylsilane (TMS). Chemical shifts are reported in ppm (parts per million) and, other than the resonance frequency, are comparable between devices.

The chemical shift is not the same for a given chemical element, but depends on the environment of its nucleus. In other words, the shift of hydrogen next to oxygen differs from that next to

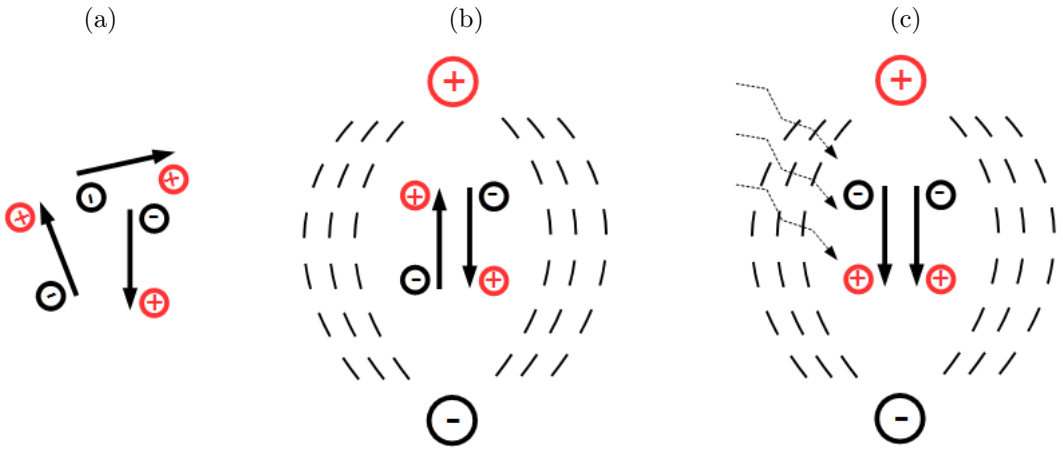

Figure 4: Nuclear spins - (a) Each atom with an odd mass or atomic number has a nuclear spin other than 0. (b) If a magnetic field is applied, the particles with nuclear spins are aligned. This can be either with the field (low energy state) or against the field (high energy state). (c) If a radio wave with energy corresponding to an atoms Larmor frequency is applied, the nuclear spin will change its direction and fall into the high energy state. When the radio wave is canceled, the nuclear spin will fall back into its low energy state, therby emitting energy that can be measured.

carbon (see figure 5). Moreover, chemical shifts are characteristic for specific functional groups or amino acids residues.

In NMR spectroscopy nuclei are measured simultaneously. This means that information gathered reflects the average of structural conformations of a molecule present in a solution. Thus, if some conformations are very rare, they may not be traceable.

1.5.1 HSQC

HSQC (Heteronuclear Single-Quantum correlation) is used to correlate 2 nuclei of different atoms in an NMR experiment. Thus, HSQC measurements are 2-dimensional NMR experiments, giving information of two different atomic nuclei at once. Correlation of ^{15}N (or ^{13}C) and protons (^{1}H) is very useful in structural studies of biological molecules. In a simplified way, the method works by applying a series of pulses to magnetize the first nucleus and transferring this magnetization to the second nucleus where the signals are detected (as oscillating voltage) and stored. For the final calculations it is however necessary to repeat the 4 step procedure a number of times (usually one hundred to a few hundred):

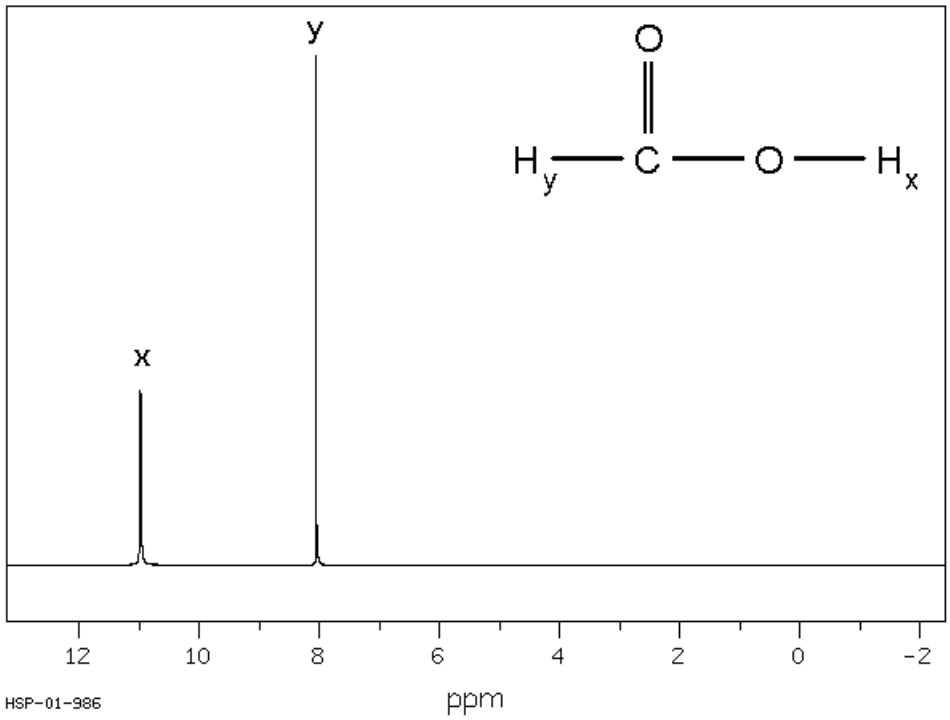

Figure 5: Example of an 1-dimensional NMR spectrum - Signal intensities vs chemical shifts are plotted for formic acid. The different chemical shifts for the two hydrogen atoms arise from the different chemical environments. While H_x is affected mainly by the oxygen it is attached to, H_y is mostly influenced by the carbon. (SDBSWeb : http://sdbs.db.aist.go.jp)

Preparation: The first type of nuclei (^{15}N for example) are exited, typically with a set of pulses that generate transverse magnetization. This can be imagined as pushing a spinning gyroscope. It will keep spinning but in a more tilted position, like the Earth does (this is called precession). However, the pulses do not only induce increased precession but also align the spins of the nuclei, so that they are in phase (see figure 6).

Evolution: The evolution period is a variable time period in which the signal evolves. This time period is incremented with each experiment in the series. It has an influence on the detected signal and is necessary to acquire the first component of the relaxation time (t_1).

Mixing: In the mixing period the magnetization is transferred from the first to the second nucleus (from ^{15}N to ^{1}H for example). This is done by another series of pulses on both types of nuclei.

Detection: In the last step, signals (Free induction decay, FID) are detected (the rotating spins induce an oscillating voltage in a coil) and stored with the evolution time for the current experiment (see figure 6). Each FID depends on the relaxation from the induced precession (with its relaxation time given by t_1) and the dephasing of the spins that constitutes the second component of the relaxation time (t_2). After the series of experiments is finished, the time-domain signals are processed by Fourier transformation to acquire frequencies and chemical shifts.

Only signals of directly adjacent atoms can be identified. The resulting HSQC spectrum is usually displayed as contour plot (see figure 7 for an example), where chemical shifts of one atom (for example ^{15}N) are plotted against the chemical shifts of the second atom (for example ^{1}H). These plots have unique patterns for different proteins and are often referred to as protein fingerprints. Although the peak intensities in such contour plots are encoded as rings (like heights in a hiking map) it is often advantageous to plot signal intensities vs. amino acids to have a better view on intensity differences.

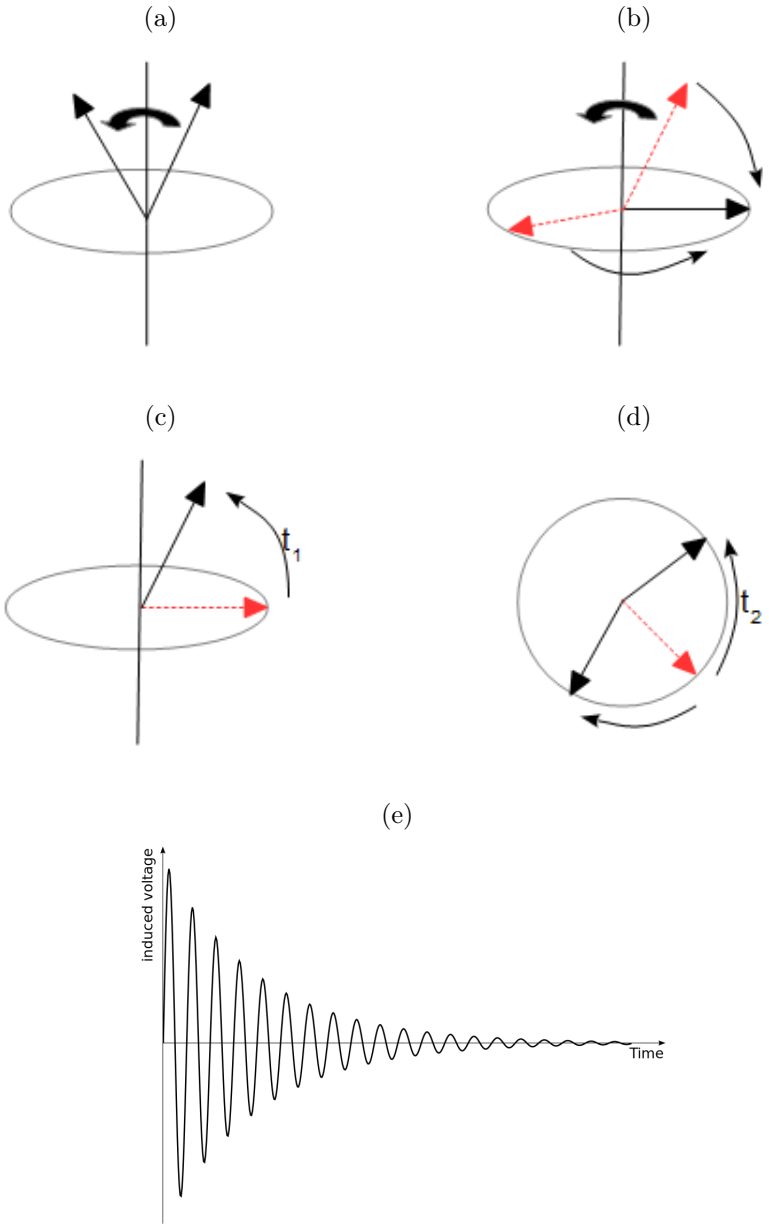

Figure 6: Relaxation time - (a) A spin that aligns in a magnetic field is not exactly aligned parallel (or anti-parallel) but develops a precession. With the right pulse sequence transverse magnetization can be generated that forces the spins of distinct nuclei to align perpendicular to the magnetic field and causes them to rotate in a circle (b). Moreover, the nuclear spins are also forced to align in phase. After the spins are aligned their relaxation can be measured. The relaxation time has two components: The first part is the relaxation from the transverse magnetization (t_1) that leads to a decay of signal intensity of the FID (c). The second part is the dephasing of the aligned spins of nuclei (t_2) that leads to a broadening of the peaks of the FID (d). Figure (e) shows an FID.

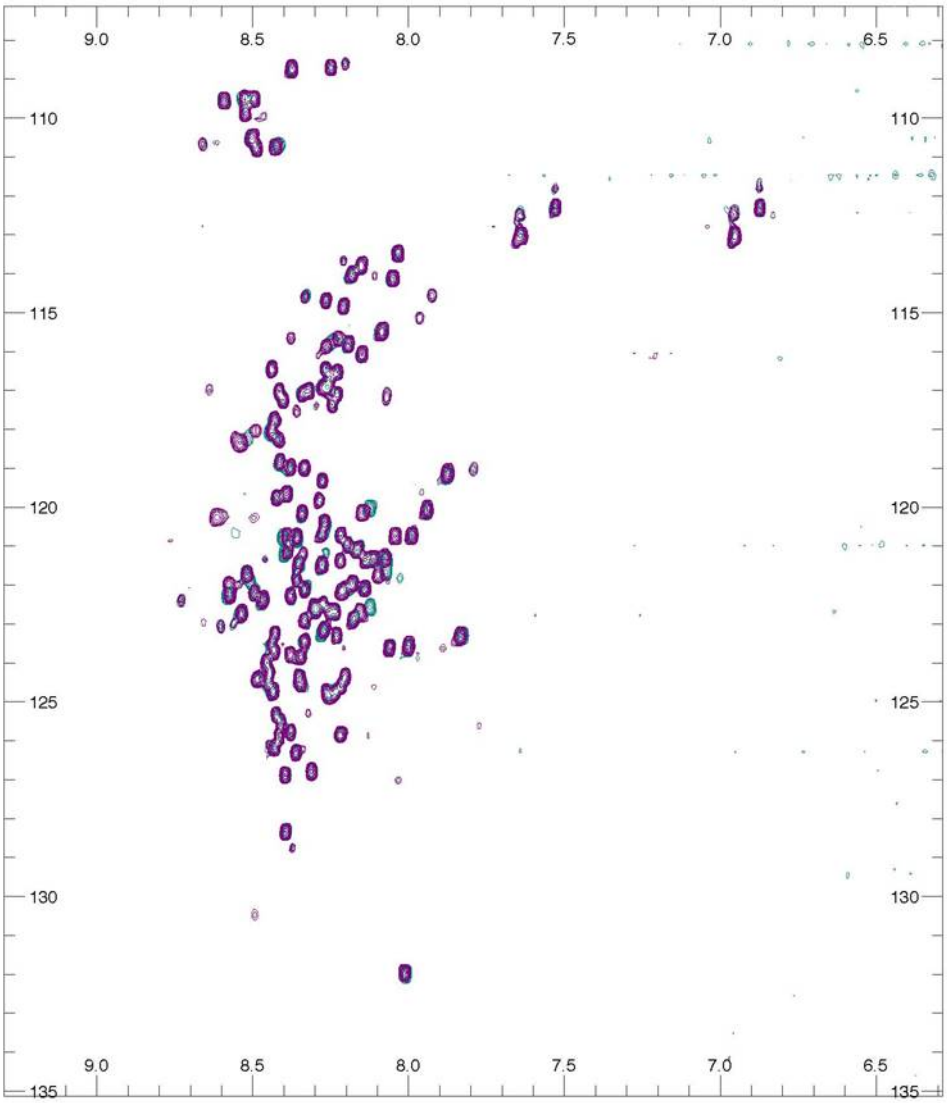

Figure 7: A 2-dimensional NMR spectrum of LC1-MTB - The plot shows the ^{1}H shifts on the abscissa and ^{15}N shifts on the ordinate. Each contour ring corresponds to an adjacent pair of atoms. Some of the amino acids can be assigned directly by looking at the plot. Glycines are clustered on the very top, asparagines and glutamines to the right. Moreover, 2-dimensional NMR spectra show specific patterns for different proteins.

1.5.2 PRE

In the para-magnetic relaxation enhancement (PRE) experiment a spin label is used to quench the electron magnetic resonance of other atoms in close proximity (up to 20 Å). The resulting data can be used to enhance the structure model of a protein. The method works by increasing the relaxation of a given atom, excluding it from the detection window. Hence, in an NMR spectrum the intensities of peaks will decrease (in contrast to a reference) for amino acids in a certain distance to the label.

A commonly used site directed spin label is MTSL, or (1-Oxyl-2,2,5,5-tetramethyl-3-pyrolin-3-yl)methyl methanthiosulfonate. It reacts very specific with sulfhydryl groups resulting in a disulfid bond linking the label and the target molecule. Hence, it can be used to tag cysteine side chains in proteins very specifically. To have tags only on defined positions the protein has to be free of cysteine in its native state (or has to have a lone cysteine on the desired spot). Hence, a single defined position (altered by mutation) can be tagged. The tag works by changing the electron para-magnetic resonance of surrounding atoms in proximity for distances up to 20 Å. As reference the tag can be either cleaved by reduction with DTT or simply be quenched with ascorbic acid.

1.6 Previous results

Recently, LC1-MTB has been examined in more detail. Meta structure analysis as well as the ^{1}H-^{15}N HSQC spectrum suggest an intrinsically disordered region at the microtubule binding domain compared to the more structured appearance at the COOH terminus. Additionally, secondary chemical shifts underline these findings and show merely a slight inclination towards an α-helix at the NH_2 terminus. [44]

A prediction based on those results is shown in figure 8.

In the past few years the idea of distinct structures necessary for specific functions had to be reconsidered, due to the increasing number of proteins lacking a well developed 3D structure. The importance and frequency of these intrinsically disordered proteins (IDPs) had been underscored [45, 46]. Each IDP forms an ensemble of very flexible, rapidly alternating structures, thus making NMR spectroscopy a favourable tool to determine structural preferences [47].

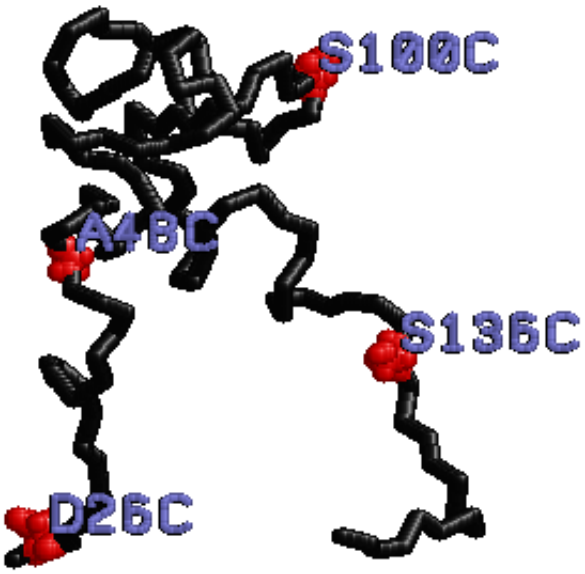

Figure 8: LC1-MTB structure prediction - The prediction is calculated from previous data aquired through backbone assignment and metastructure analysis. The 4 mutations mentioned in chapter 1.7 are shown. Note that the 6xHIS-tag is not included in this figure, although the labelling corresponds to the protein including the His-tag (for consistency).

As mentioned earlier, the LC1-MTB appears to have an intrinsically disordered character itself [44]. Thus, NMR could reveal more detailed structural information, lead to insights about the existence of secondary structure elements and may reveal the underlying mechanism of microtubule binding.

1.7 Project overview and goals

Our main goal was to get a more detailed view on the structure of LC1-MTB. For this purpose, we expressed ^{15}N wild-type (wt) LC1-MTB and did ^{1}H-^{15}N HSQC experiments with the wt free in buffer, bound to microtubules and bound to tubulin. To confirm these results competition with ^{14}N wt in microtubule binding was introduced. Furthermore NMR PRE experiments were done, to gain information on spatial distances between parts of LC1-MTB. Therefore, 4 single missense mutations were introduced in the wt sequence to change respective amino acid residues to cysteines. After protein expression, these cysteines were tagged with MTSL

and measured free in buffer, bound to microtubules or bound to tubulin. Finally, to see if distances between neighbouring LC1-MTBs bound to microtubules or tubulin are short enough for intermolecular PRE to be observed, we did measurements with ^{15}N wt, MTSL-tagged ^{14}N mutants and microtubules or tubulin.

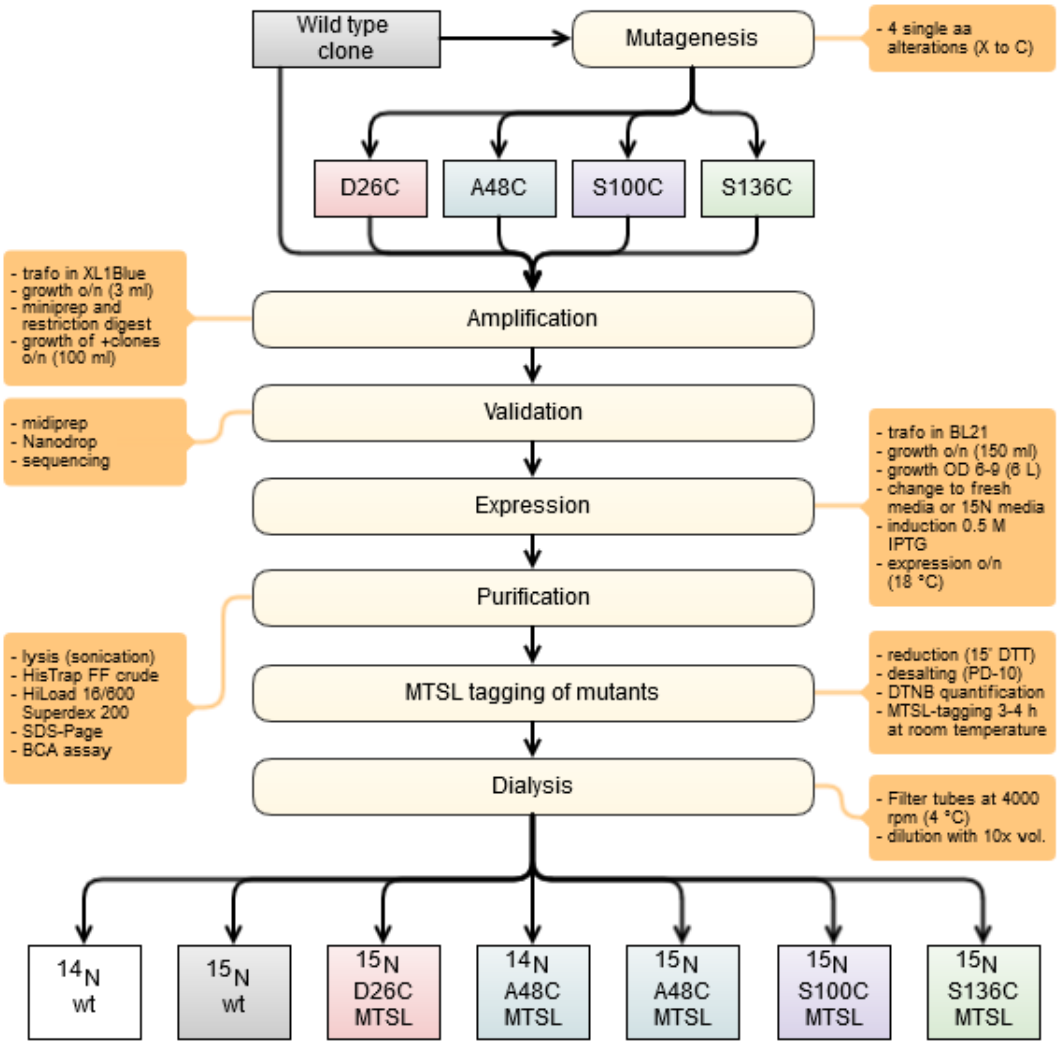

Figure 9: Expression and purification workflow - The overview shows the processing of clones and proteins before NMR spectroscopy. The squares represent different samples, the rounded rectangle illustrate processes and the arrows show the sequence. Bubbles connected to the processes show some detail about the procedures. All mutants were validated by DNA sequencing and expressed in presence of a ^{15}N ammonium source. Additionally, they were MTSL-tagged and dialysed. Wt was expressed with ^{15}N ammonium and as a standard ^{14}N protein. Additionally, A48C was expressed as a standard ^{14}N protein and MTSL-tagged.

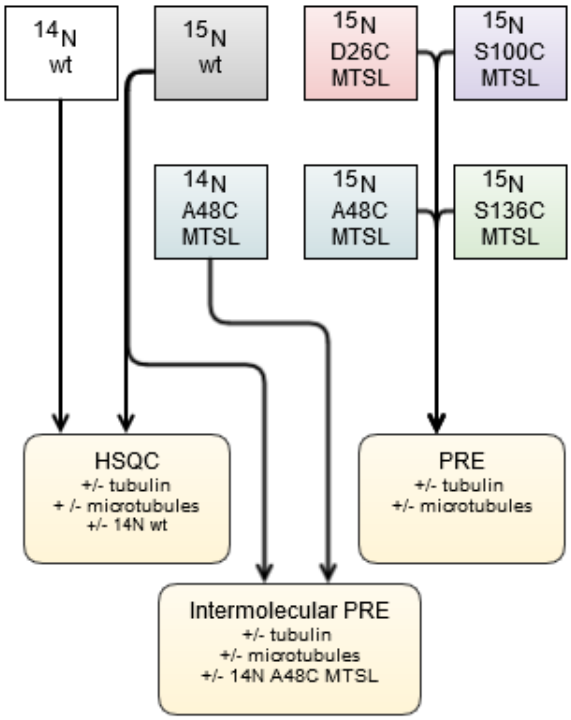

Figure 10: NMR spectroscopy overview - The different NMR spectroscopy set-ups and which samples were used in the different experiments is shown. PRE was planned with all the mutants with and without microtubules or tubulin. Standard HSQC was only done with ^{15}N wt and in the presence or absence of microtubules or tubulin. As control ^{14}N wt was added to check for competition in microtubule and tubulin interaction. Furthermore, intermolecular PRE was done with ^{15}N wt and MTSL-tagged ^{14}N A48C in the presence or absence of microtubules or tubulin.

2 Materials and methods

2.1 Cloning

Wt clones were obtained by insertion of the NH_2-terminal microtubule binding domain of LC1 (amino acids 2212 to 2338 of the MAP1b precursor; see sequence in table 1) from *Rattus norvegicus* into a pet-15b expression vector. Hence, a 6x HIS-tag was added at the NH_2 terminus of the sequence. This was verified with 2 standard sequencing reads (VBC-Biotech) done with T7-promoter and T7-terminator primers (see table 1).

4 separate mutations were introduced to change the amino acids on positions 26 (aspartic acid), 48 (alanine), 100 (serine) and 136 (serine) to cysteine. This was done with the *QuikChange Site-Directed Mutagenesis Kit* from *Stratagene*. Primers used for the mutagenesis are shown in table 1.

Wt coding sequence	
MGSSHHHHHHSSGLVPRGSHMEFMVDPEALAIEQNLGKALKKDLKEKAKT KKPGTKTKSSSPVKKGDGKSKPSAASPKPGALKESSDKVSRVASPKKKES VEKAMKTTTTPEVKATRGEEKDKETKNAANASASKSVKTATAGPGTTKTA	
Cloning primers	
D26C	CCATATGGAATTCATGGTGTGTCCAGAGGCCTTGGC GCCAAGGCCTCTGGACACACCATGAATTCCATATGG
A48C	GGATCTGAAGGAGAAGTGCAAGACCAAGAAACCAGGC GCCTGGTTTCTTGGTCTTGCACTTCTCCTTCAGATCC
S100C	GGCTTCTCCCAAGAAGAAAGAGTGTGTGGAGAAAGC GCTTTCTCCACACACTCTTTCTTCTTGGGAGAAGCC
S136C	GCTTCTGCATCCAAGTGTGTGAAGACTGCAACAGCAG CTGCTGTTGCAGTCTTCACACACTTGGATGCAGAAGC
Sequencing primers	
T7-promotor	TAATACGACTCACTATAGGG
T7-terminator	GCTAGTTATTGCTCAGCGG

Table 1: Cloning and sequencing - The table shows the coding sequence of LC1-MTB. Additionally, the primers used to generate the 4 mutants and sequencing primers are listed.

QuikChange Kit

The kit makes use of a high fidelity DNA polymerase (PfuTurbo) and DpnI, an endonuclease degrading only methylated and hemimethylated DNA. A PCR is done with the original DNA fragments and primers containing a desired variation to accumulate altered daughter strands. Afterwards DpnI is added (1h at 37 °C) to digest methylated/hemimethylated - hence parental - DNA, leaving only daughter strands. The remaining mutated plasmids are transformed into *E. coli* XL-1 blue for amplification and selection (see figure 11).

2.1.1 Transformation

For transformation a tube with 20 µl KCM (0.5 M KCl, 0.15 M $CaCl_2$, 0.25 M $MgCl_2$), 25 µl of plasmid DNA and 55 µl ddH_2O was prepared and cooled down on ice. 100 µl of KCM competent *E coli* XL1 blue were thawed, added to the preparation and incubated on ice for 20 min. Another 5 min of incubation on 37 °C was done and 1ml LB (pre-warmed to 37 °C) was added, followed by 45 min incubation on 37 °C while shaking. Afterwards the transformed bacteria were spread out on an 100 mm agar dish (including ampicillin) and incubated on 37 °C over night. The next day, colonies were inoculated in 3-4 ml of LB with ampicillin and incubated again over night at 37 °C while shaken at 180 rpm.

2.1.2 Plasmid extraction

The next morning, minipreps were started by pouring about 1.5 ml of each overnight culture into a microcentrifuge tube followed by 1 min centrifugation at maximum speed (Eppendorf 5415C, 16,000 g). The supernatant was removed, the pellet resupended in 200 µl of solution P1 (50 mM Tris/HCL, 10 mM EDTA, pH 8.0, 100 µg/ml RNAse) and incubated for 5 min. 200 µl of solution P2 (0.2 M NaOH, 1 % SDS) were added and the tube inverted 2 times. After about 3 to 5 min on ice 200 µl of solution P3 (3 M KAc, 2 M HAc, pH 5.5) were added and the tube inverted 20 times. Another 5 min on ice was followed by 5 min of centrifugation at maximum speed (Eppendorf 5415C). The clear supernatant was mixed with 1 ml 95 % ethanol and stored at -20 °C for 20 min followed by centrifugation at maximum speed (Eppendorf 5415C) for 30 min. The supernatant was removed and 500 µl 70 % ethanol were added to the pellet. After

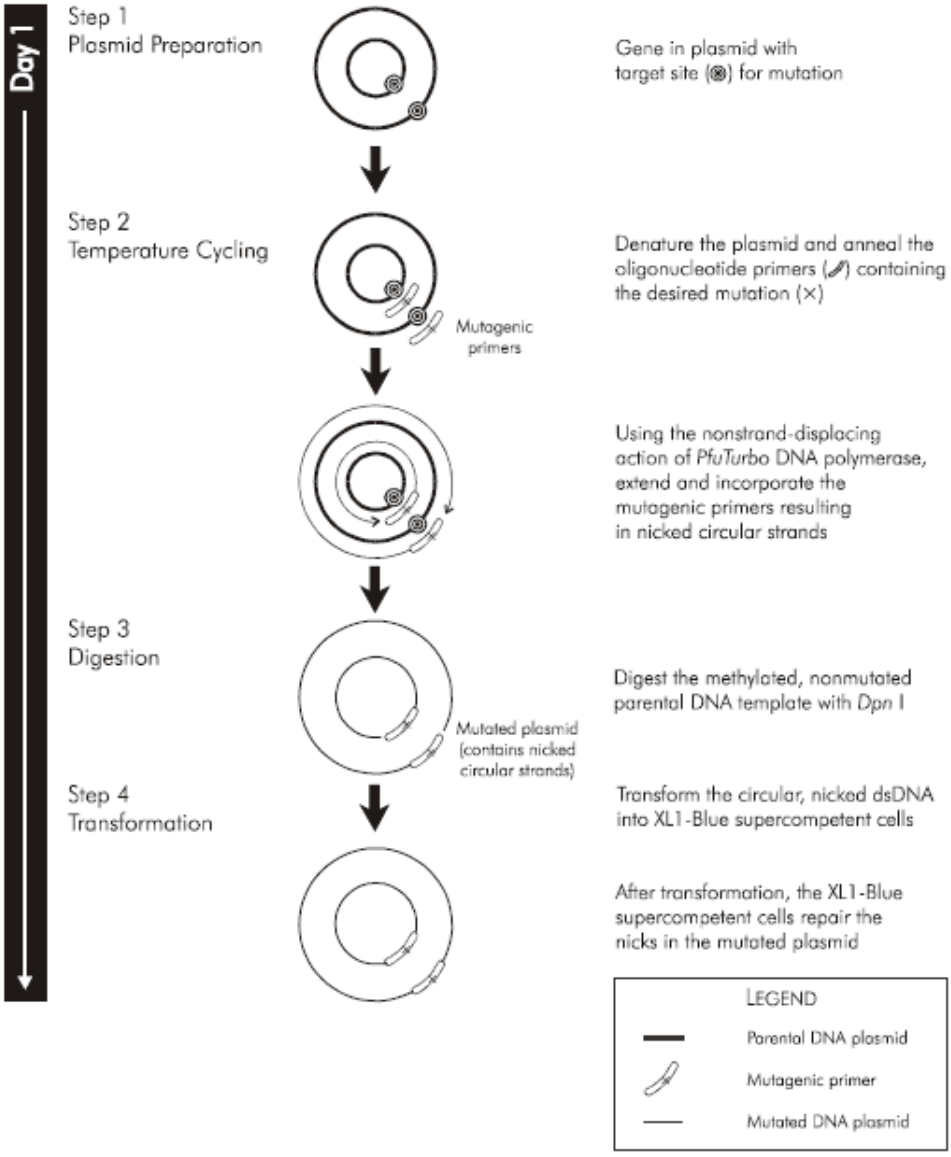

Figure 11: QuikChange mutagenesis overview - The QuikChange mutagenesis kit works by standard PCR mechanisms followed by selective degradation of template (parental) DNA-strands. (QuikChange mutagenesis kit instruction manual, Stratagene).

1 min of centrifugation at max. speed the supernatant was removed and the pellet dried for several minutes (at 55 °C). The dry pellet was re-suspended in 30 µl buffer TE.

2.1.3 Amplification

For an initial check if the cloning worked correctly 25 µl of each sample were digested with BamHI and EcoRI for 1 h at 37 °C and applied to a 1.2 % agarose gel. For size estimation the GeneRuler 1 kb DNA Ladder (Thermo Scientific) was used. For visualization of sample DNA we used Ethidium bromide and UV light. Electrophoresis was carried out at 120 V for approximately 30 min. After gel electrophoresis 3 to 5 samples were chosen among those showing the correct fragment size, and 2 ml of each broth was added to 100 ml LB with ampicillin and incubated over night at 37 °C.

Agarose gel electrophoresis

The method works by pulling negatively charged DNA fragments (the negative charge originates from the sugar phosphate backbone) in an electrical field towards a positive electrode. To not simply move the DNA fragments but separate them by size a gel is added between the electrodes. The gel itself consists of agarose dissolved in a conductive buffer by cooking. For visualization of DNA a dye is mixed into the gel, getting incorporated into the fragments while they are pulled through. The liquid gel is poured into a container and a comb is added to create loading pockets for the samples. After cooling the gel builds a mesh-like structure. While smaller fragments may pass the mesh nearly unhindered, bigger fragments are retarded corresponding to their size, thus leading to the separation of the DNA applied to the gel. The gel is placed into a tank, surrounded by the same buffer used to cast it, to provide contact with the electrodes. DNA samples are prepared by mixing them with appropriate loading buffers, containing a dye to see roughly how far the gel has run and something to render the sample more dense than the running buffer (usually glycerol), thus preventing the sample from defusing out of the pockets. To estimate the size of specific fragments not only unknown samples but a DNA mix with fragments of known size (DNA ladder) may be applied to each electrophoresis run (see figure 12).

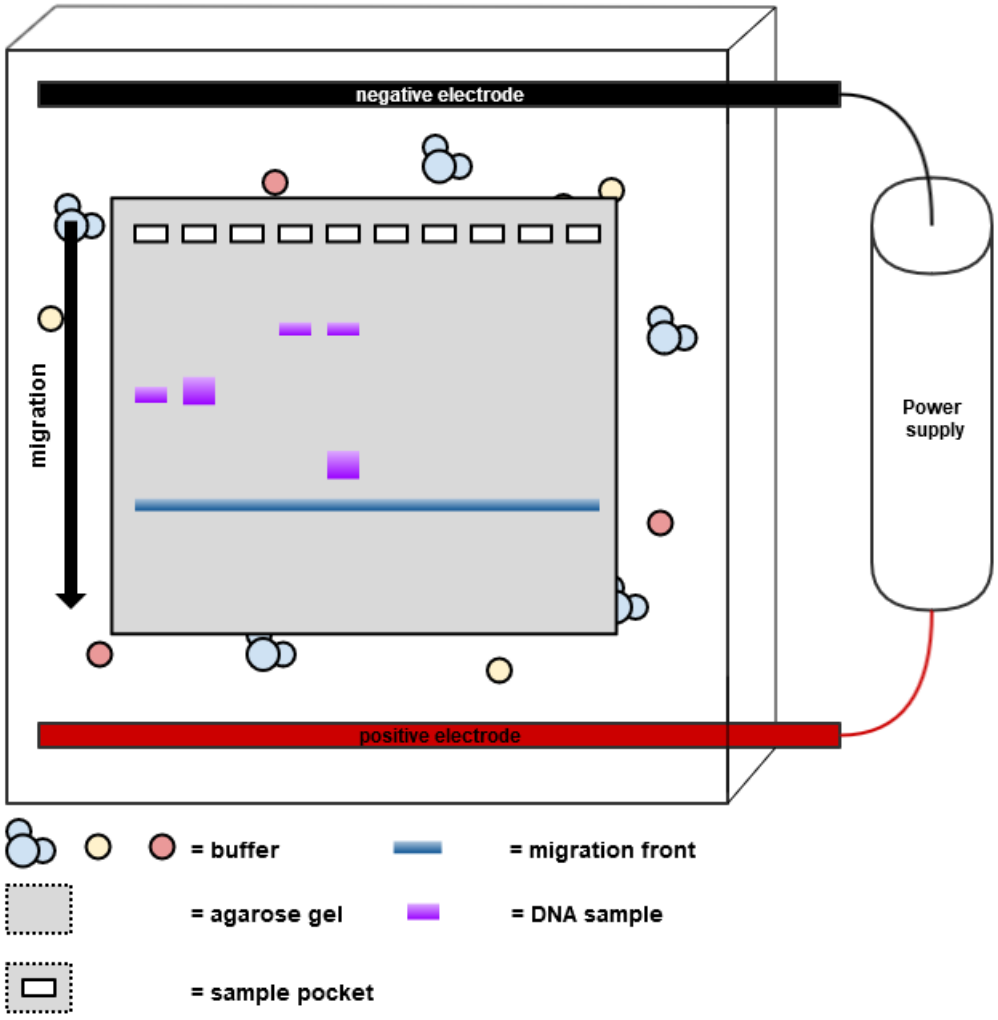

Figure 12: Gel electrophoresis schematics - In an agarose gel electrophoresis the negatively charged DNA migrates through the gel in direction of the positive electrode. The loading buffer contains a dye showing how far the particles have migrated (blue line). The size of the DNA-fragments can be estimated by the distance they have moved (for size approximations a DNA ladder mix containing fragments of defined size is compared to sample fragments). The fluorescence intensity of a given fragment is proportional to its amount, thus quantification is possible if compared to samples of known concentrations.

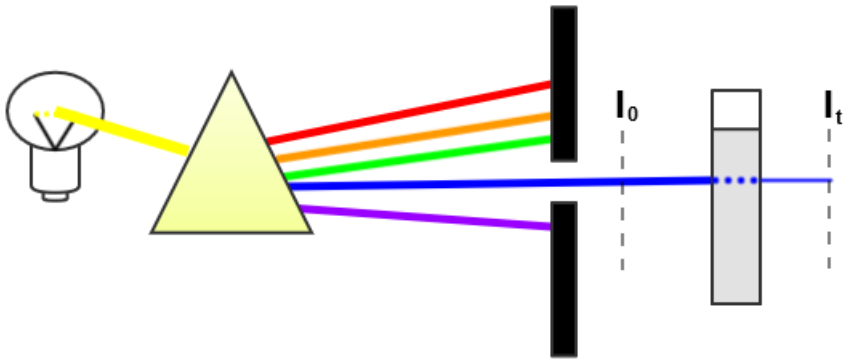

Figure 13: Spectrophotometry - Light from a light source (emitting white light in this example) is split up by a prism (or grating) into different wavelengths. Only wavelengths that are chosen may pass through to the sample. The intensity of the beam is measured before (I_0) and after (I_t) it penetrates the sample. Lambert Beer's law ($\log\left(\frac{I_0}{I_t}\right) = \varepsilon_\lambda \cdot c \cdot d$) can then be used to calculate the concentration with ε_λ being the wavelength dependent extinction coefficient, d being the path length and c being the concentration. Alternatively the absorbance ($\log\left(\frac{I_0}{I_t}\right)$) of a sample can be compared to absorbances of a series of protein standards with known concentrations to determine the concentration of the sample.

2.1.4 Validation

Midipreps were done from the prepared 100 ml LB broths with the *JETSTAR Plasmid Purification Kit* (Genomed) according to the manufacturer's protocol. NanoDrop was used to measure DNA concentration. 150 ng of DNA per sample were sent for sequencing (VBC Biotech). The rest was stored at 4 °C and later used for expression.

NanoDrop

NanoDrop is a spectrophotometer and therefore measures the difference in intensities before (I_0) and after (I_t) light penetrates a sample. This ratio in combination with the path length (d) and the sample dependent extinction coefficient (ε_λ) can be used to calculate the protein concentration through Lambert Beer's law ($\log\left(\frac{I_0}{I_t}\right) = \varepsilon_\lambda \cdot c \cdot d$). To get reasonable results the wavelength has to be adopted to the sample. In case of DNA (as well as RNA) a beam at 260 nm is used based on its absorbance maximum (see figure 14). In contrast to other methods NanoDrop only needs 1 µl of sample solution and can detect concentrations of a few ng/µl.

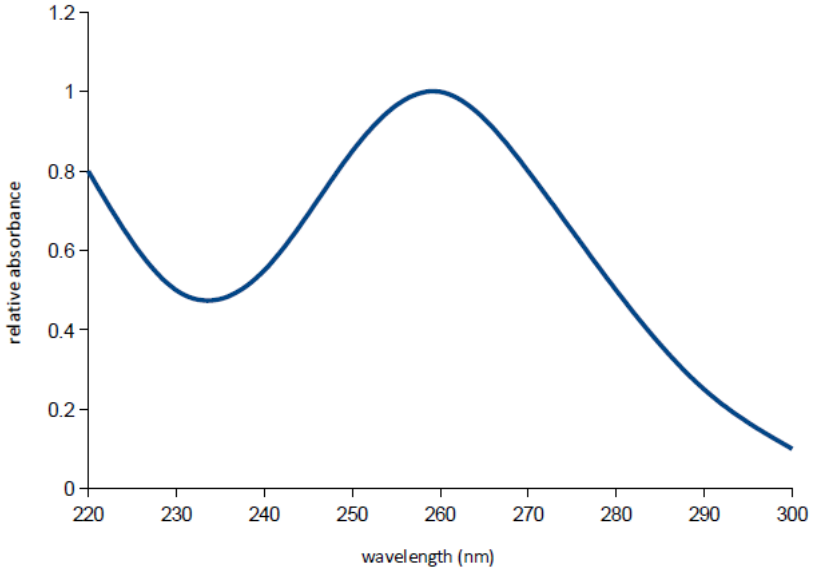

Figure 14: DNA absorbance spectrum - As shown in this example, the absorbance spectrum of DNA (and RNA) has its maximum at 260 nm.

2.2 Expression

2.2.1 Transformation

Protein expression was done in *E. coli* BL21 Codon Plus (DE3). Transformation was done by heat shock with 30 ng of vector DNA. The DNA was mixed with 100 µl of thawed competent bacteria and incubated on ice for 20 min. Heat shock was done for 30 sec at 42 °C followed by 3 min on ice. After addition of 500 µl SOC media the bacteria were incubated for 1 h at 37 °C with agitation.

E. coli BL21 Codon Plus (DE3)

Expression in *E. coli* BL21 Codon Plus is T7 promoter driven. Moreover, the strain is genetically enhanced for expression (inactivation of plasmid DNA degrading endonuclease I, etc.). In addition extra plasmids coding for arginine, tyrosine and tryptophane tRNAs are present. Those amino acids would else be the limiting factors in the expression of heterologous proteins. To ensure the extra plasmids are not lost, they contain a chloramphenicol resistance gene, providing a tool for selection.

2.2.2 Growth

50 ml LB with ampicillin and chloramphenicol were prepared and mixed with the transformed bacteria (a total of 3 50 ml cultures were done per expression). Incubation was done over night at 37 °C at 180 rpm. 6 L pre-warmed LB with antibiotics were poured into Erlenmeyer flasks and mixed with the over night cultures (2 L for each 50 ml broth). The bacteria was grown for 3-5 h to an OD_{600} between 0.6 and 0.9.

2.2.3 Induction

Before induction bacteria were spun down at 6,000 rpm (Sorvall RC5C, F10, 6,400 g) for 12 min at 4 °C and re-suspended in ¼ of the origin volume of supplemented M9 media (see table 2) containing solely ^{15}N as nitrogen source. For expression of ^{14}N proteins the pellets were re-suspended in LB media instead of M9 media. This was followed by another 1 h at 37 °C and 180 rpm. Induction was started with 0.5 M IPTG and expression done over night at 18 °C at 180 rpm.

IPTG induction

Isopropyl-β-D-thiogalactopyranosid works by inhibiting the binding of a repressor (LacI) to the lac operator. In case of T7 based expression vectors the repression is done at two sites. One lac operator is positioned between the T7 promotor and the gene of interest, blocking progression of T7 polymerase. The second is placed before the T7 polymerase gene blocking the expression of the polymerase itself. Withdrawal of the repressor starts the expression of T7 polymerase (through the bacteria's own expression system) which may then bind to the T7 promoter. Since IPTG also displaces the repressor before the gene of interest, the T7 polymerase can proceed along the gene and expression is started (see figure 15).

2.2.4 Lysis

Bacteria were harvested by centrifugation at 6,000 rpm (Sorvall RC5C, F10, 6,400 g) for 12 min at 4 °C. The pellets were re-suspended in 15-20 ml lysis buffer (50 mM NaH_2PO_4, 300 mM NaCl, 1 L ddH_2O, pH 8, degassed for 60 min) and stored at -20 °C (for at least 1 h).

(a) before IPTG induction

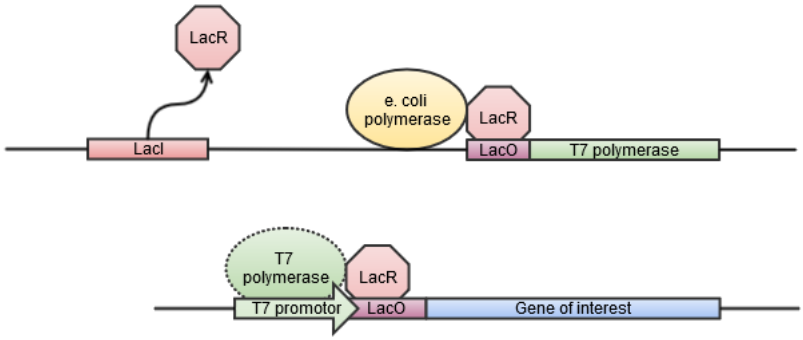

(b) after IPTG induction

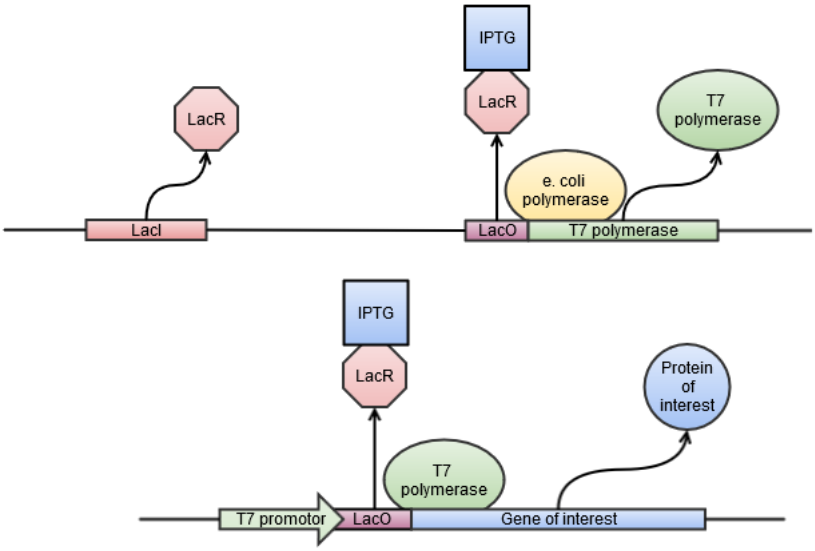

Figure 15: IPTG induction schematics - Before IPTG induction, the repressor (LacR) is blocking the path for *E. coli's* RNA polymerase, preventing the expression of T7 polymerase. Even if T7 polymerase was present, it would be blocked by another LacR before it could reach the gene of interest (a). If IPTG is added it binds LacR and releases it from the lac operator (LacO), opening the passage for RNA polymerase (b). *E. coli* RNA polymerase can therefore translate T7 polymerase, which in turn can pass though LacO and translate the gene of interest.

M9 media (supplemented)			
6 g	$Na^2HPO^4.2H^2O$		
3 g	KH_2PO_4		
0.5 g	NaCl		
1 L	ddH_2O		
1 g	$^{15}NH_4Cl$		
2 mM	$MgSO^4$		
0.4 %	glucose		
0.3 mM	$CaCl_2$		
10 ml		**trace elements**	
		5 g	EDTA
		0.83 g	$FeCL_3.6H_2O$
		84 mg	$ZnCl_2$
		13 mg	$CuCl_2.2H_2O$
		10 mg	$CoCl_2.6H_2O$
		10 mg	H_3BO_3
		1.6 mg	$MnCl_2.6H_2O$
		1 L	ddH_2O
			pH adjusted to 7.5
50 mg	ampicillin		
25 mg	chloramphenicol		
all contents either autoclaved or filtered sterile			

Table 2: M9 medium (supplemented) - The table lists the contents of the minimal medium supplemented with a ^{15}N ammonium source.

The thawed bacteria solution was supplemented with 0.002 g DNaseI, 0.08 g lysozyme and 2 EDTA-free protease inhibitor tablets (Roche). The cells were lysed by sonication (20x 10 sec at 80 %) and cooled by brief immersion of the tube in liquid nitrogen after each sonication step. Cell debris were removed by centrifugation at 13,000 rpm (Sorvall RC5C, F21s, 20,000 g) for 30 min at 4 °C and the supernatant was stored at 4 °C.

2.3 Purification

2.3.1 MAP1b light chain (NH_2 terminus)

Purification was done by FPLC (Fast protein Liquid Chromatography) in 2 steps. An Äkta FPLC (GE Healthcare) was used for both the affinity and the size exclusion step. Affinity purification was done with a prepacked HisTrap FF Crude 5ml column (GE Healthcare) loaded

with Ni^{2+}. Gel filtration was done with a prepacked HiLoad 16/600 Superdex 200 column (GE Healthcare). In the affinity step, loading was done with the sample pump at 1 ml/min followed by washing with lysis buffer. Elution was done in 3 consecutive steps with lysis buffer and increasing imidazol concentrations (20 mM, 75 mM and 500 mM). All buffers and solutions were degassed for 1 h before they were applied to the machine. SDS PAGE was used to determine the protein fractions and to estimate the purity of the protein. The purest fractions were applied to the Superdex column using a 2.5 ml loading loop. Therefore the samples were concentrated to roughly 2 ml with centrifugal filter units (Amicon Ultra-15 centrifugal filter units, 10,000 NMWL) and injected into the loop. The purification was done at 1 ml/min with lysis buffer. 1 ml fractions were collected and checked for protein purity and concentration via SDS PAGE and BCA protein assay, respectively. SDS PAGE was done using 12 % gels at 25 mA per gel. *PageRuler Prestained Protein Ladder* (Thermo Scientific) was used as marker. The *BCA protein assay kit* (Thermo Scientific) was used according to the manufacturers recommendations. The best fractions were combined, concentrated to 2 ml, frozen in liquid nitrogen and stored at -80 °C.

Affinity chromatography

In affinity chromatography a sample solution is pumped through a column filled with beads containing a binding partner. Depending on the protein of interest different binding partners can be chosen to be immobilized on the beads. While the solution flows through the column the protein binds to the beads (respectively its binding partner) and is trapped. The remaining substances in solution may exit the column and be collected as flow through. To elute the trapped protein either a change in pH, ionic strength or a competing binding partner can be used (see figures 16a and 16b).

Gel filtration/Size exclusion chromatography

Gel filtration separates molecules based on their size. Columns are filled with media consisting of particles forming a porous matrix. The bigger a molecule is the worse it fits through the different pores and the faster it moves through the column. In contrast the smaller a molecule is the more pores it can enter and thus its progress through the column is retarded. Hence,

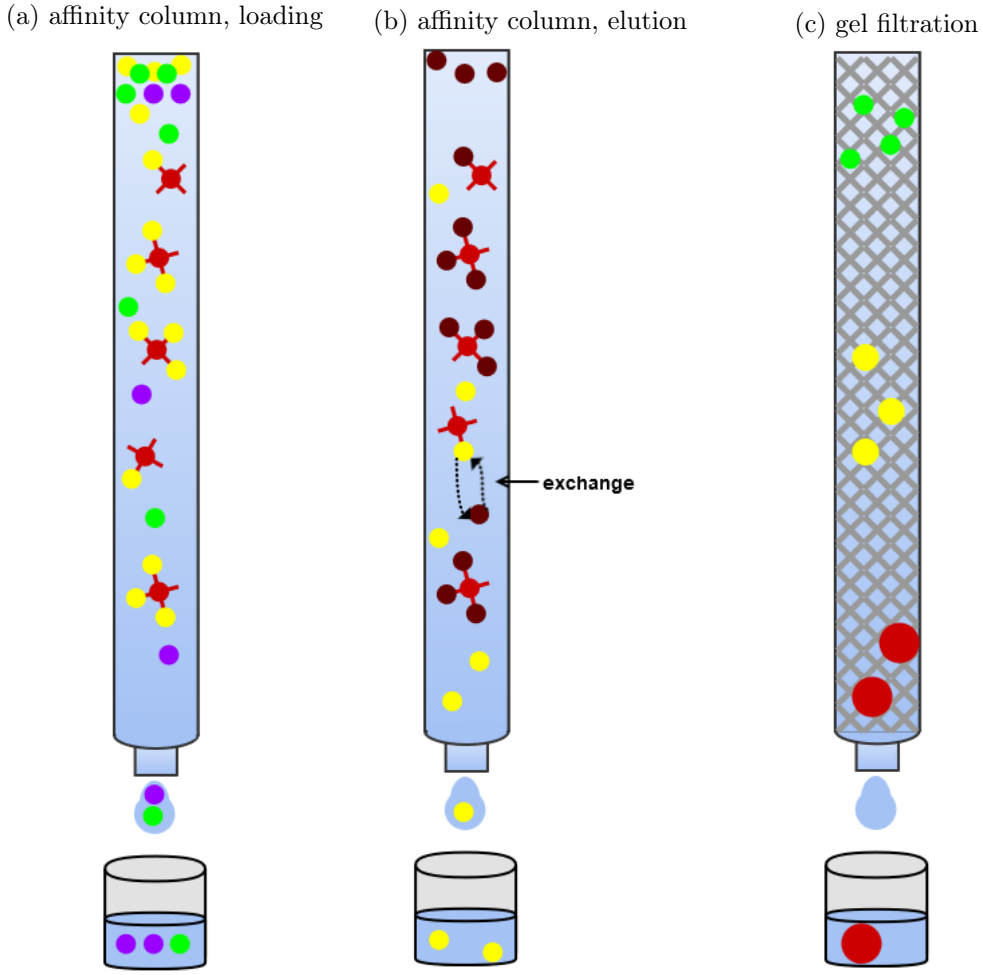

Figure 16: Chromatography - (a) In affinity chromatography beads linked to a ligand (red) are immobilized on a column. A solution including the protein of interest (yellow) is either actively (with a pump) or passively (by gravity) applied to the column. While the protein of interest binds to its binding partner (ligand) and is immobilized, all the other compounds of the solution flow through and exit the column. After the sample is applied buffer is pumped though the column to wash out all remaining unbound molecules. (b) Elution is done either by a change in pH, ionic strength or a competing binding partner for the ligand. When a buffer including a competitor (brown) is pumped through the column, the protein of interest and the competitor are exchanged. The protein of interest is released into the mobile phase and can be collected as it exits the column. (c) In size exclusion chromatography the molecules are delayed based on their size. The better they fit between the pores of the matrix, the longer they need to migrate through the column. Thus, the bigger a molecule, the faster it exits the column.

molecules of various sizes move with different velocities through the column and are separated from each other (see figure 16c).

SDS PAGE

SDS PAGE (sodium dodecyl sulfate polyacrylamide gel electrophoresis) is used to separate proteins by their size. As in agarose gel electrophoresis an electrical field is applied providing the force for charged molecules to move through a gel. The gel itself acts as a mesh delaying the movement of bigger molecules in proportion to their size. The gel consists of acrylamid (forms polymers), bisacrylamid (cross-links acrylamids polymers), SDS (a denaturing agent) and a buffer. Those components are mixed together in concentrations depending on the experiment. In general the ratio bisacrylamid/acrylamid is about 1:30 or 1:35. The percentage of the gel however has to be fitted to the molecular weight of the samples and may vary from 4 % up to 25 %, with the higher percentage (narrower mesh) for separation of smaller molecules. Before samples are applied to the gel they are mixed with a sample buffer (Laemmli in many cases). It consists of a buffer (to adjust the pH), a dye (to see the front while running), some reagent to reduce disulfid bonds (DTT, 2-Mercaptoethanol, etc.), glycerol (to weigh the sample down) and SDS. Since proteins have different charges depending on their primary structure, they would all behave very differently in an electrical field. SDS denatures proteins to more or less unfolded chains and unspecifically binds along the protein chain through its hydrophobic moiety, thereby assigning its own negative charge proportional to the size of the protein. Hence, every polypeptide sustains roughly the same ratio of molecular mass to charge, allowing separation in a field to occur solely on size. After mixing the sample with a sample buffer the solution is heated at 70-100 °C for 5 to 10 minutes (the lower the temperature the longer the incubation) to enhance denaturation and either stored (at -20 °C) or directly applied to a gel. After the electrophoresis is finished the proteins in the gel can be stained with Coomassie Brilliant Blue (or other dyes) to reveal the protein bands (see figure 12 for electrophoresis).

BCA protein assay

The BCA protein assay is a colorimetric method used to determine protein concentration. It combines a reduction of Cu^{2+} to Cu^{1+} and a reaction of Cu^{1+} with bicinchoninic acid (BCA). The result is a purple colored complex mainly due to the presence of cysteine, tryptophan and tyrosine. The complex absorbs light with a maximum at 562 nm, hence spectrophotometry is done at this wavelength. The concentration of a protein lysate can be obtained by comparing the absorbance of the lysate to a standard curve of samples of known concentrations (bovine serum albumin in most cases). See figure 13 for details on spectrophotometry.

2.3.2 Tubulin

Tubulin was purified from porcine brain. The brains from freshly slaughtered pigs (about 1 kg) were put in a plastic bag on ice immediately with 1 L carrying buffer (300 mM Sucrose, 1 mM EGTA, spatula tip of PIPES, 1 L ddH_2O, pH 7) poured over them. A 1 L beaker was filled with 100 ml of cold extraction buffer (0.5 M Sucrose, 1mM EGTA, a spatula tip of PIPES, 1 L ddH_2O, pH 7). Blood clots, vessels, connective tissue and white matter were removed and the remaining grey matter collected in the beaker. The weight of brain tissue was determined and volume of extraction buffer was adjusted to 1 ml buffer for each 1 g of tissue. After addition of 1 mM ATP and 0.1 mM GTP (final concentration) the tissue was minced with a blender 3 times for 10 sec. The tissue was further disrupted in a glass-teflon-homogenizer with 5 strokes while rotating at low speed. The suspension was centrifuged at 75,000 g for 60 min at 4 °C. The supernatant was decanted and ⅒ of the total volume of 10x PIPES buffer (1M PIPES, 10 mM EGTA, 10 mM $MgCl_2$, pH 7) was added. 3.5 M Glycerol (roughly ⅓ of the total volume), and 0.1 mM GTP (final concentration) were added and the extract incubated at 37 °C for 45 min. Centrifugation was done at 75,000 g for 90 min at 37 °C. After measuring the volume the supernatant was discarded and the pellet re-suspended in 1x PIPES buffer (¼ of the discarded supernatant's volume). 1 mM GTP (final concentration) was added and the suspension was incubated at 4 °C for 45 min while homogenizing in a glass tissue grinder with 3 gentle strokes every 10-15 min. Following centrifugation at 75,000 g for 1 h at 4 °C the supernatant was collected. 3.5 M glycerol and 0.0035 volumes of GTP (100 mM) were added and the solution was incubated at 37 °C for 45 min. Centrifugation at 75,000 g was done for 1 h at 37 °C, the

supernatant discarded, pellets frozen in liquid nitrogen and stored at -80 °C. Our preps yielded 4 pellets with about 20-40 mg each.

For further purification of each pellet a column with phosphocellulose P-11 (PC) was prepared. 20 g of PC was suspended in 1.5 L of 50 % ETOH and rocked for 30 min followed by 5 minutes rest. The supernatant was discarded and the PC washed 3 times with ddH_2O. 2 cycles of suspension in 1.5 L of 0.5 M HCL were done while rocking for 30 min each, with sedimentation/washing steps (5 min settling down, 3 times ddH_2O) in between and afterwards. Suspension in 1.5 L of 1x PIPES buffer for 20 min with agitation was done. The pH was adjusted to 6.1 with NaOH and the PC agitated for 2 h. After 5 min rest the buffer was changed and the suspension rocked over night at 4 °C.

The next day a column was filled with the phosphocellulose and equilibrated with 1x PIPES buffer for 1 h. A microtubule pellet was thawed and suspended in 1x PIPES buffer (concentration of about 15 mg/ml). 1 mM GTP (final concentration) was added and the solution incubated in a glas homogenizer for 1 h with gentle strokes every 10-15 min. Centrifugation at 75.000 g for 30 min at 4 °C was done and the supernatant decanted. 1 mM GTP (final concentration) was added and the solution was incubated at 37 °C for 45 min. Centrifugation at 75,000 g for 30 min at 37 °C was followed by re-suspension of the pellet in 1x PIPES buffer (concentration of about 10 mg/ml) containing 1 mM GTP. Another homogenization step for 30 min on ice was done, followed by centrifugation at 75.000 g for 30 min at 4 °C. The supernatant was loaded onto the equilibrated PC column. Elution was done by gravity flow with 1x PIPES buffer. Fractions of 500 µl were collected and checked instantly for presence of protein with Bradford reagent (at this point only a quick check for color change was done). An aliquot was taken from each protein fraction and the fractions were frozen in liquid nitrogen immediately. The fractions were stored at -80 °C and an SDS PAGE (see 2.3.1 SDS PAGE) as well as a Bradford assay were done.

Phosphocellulose (P-11)

Phosphocellulose is a cation exchange resin for ion exchange chromatography. The method works similar to affinity chromatography (2.3.1 Affinity chromatography) but depends on opposing charges on resin and sample molecules. While oppositely charged molecules are bound,

neutral and equally charged molecules stay in the mobile phase and exit the column. Elution is done by replacing the sample molecule with a molecule of the same charge thereby exchanging them and releasing the sample with the flow through.

Bradford protein assay

The Bradford assay is a colorimetric method like the BCA protein assay (see 2.3.1 BCA protein assay). The method is based on the binding of Coomassie brilliant blue G-250 dye to arginine, histidine, phenylalanine, tryptophan and tyrosine. Binding changes the absorbance maximum of the dye from 470 nm (in the free form) to 595 (in the bound form) resulting in an immediate colour change from brown to blue. This happens very rapidly (in a matter of seconds), thus the method can be used for very quick controls. To obtain the accurate concentration the absorbance of the sample has to be fitted to a standard curve of reference samples of known protein concentrations (see figure 13 for spectrophotometry).

2.4 NMR measurements

Dialysis with MT assembly buffer (100 mM Pipes, 1 mM EGTA, 1 mM $MgCl_2$, pH 6.8) was performed on all samples prior to NMR measurements to unify salt concentrations and pH values. This was done with centrifugal filter units (Amicon Ultra-15 centrifugal filter units, 10,000 NMWL) by centrifugation at 4000 rpm (Heraeus Megafuge, 3000 g) at 4 °C. Samples were first concentrated to 3-5 ml and diluted with 10 times the volume, spinning at 4000 rpm (Heraeus Megafuge) in between. The following experiments were done on Agilent Direct Drive 600 and 800 MHz spectrometers:

- HSQC measurements of ^{15}N wt
  - on its own (only as reference)
  - with polymerized microtubules (followed by competition with ^{14}N wt)
  - with unpolymerized tubulin
- PRE measurements of MTSL-tagged ^{15}N mutants (26, 48, 100 and 136)
  - on their own

  - with polymerized microtubules
  - with unpolymerized tubulin
- Intermolecular PRE measurements of MTSL-tagged ^{14}N A48C and ^{15}N wt

2.4.1 HSQC ^{15}N wt with polymerized microtubules (with or without competition)

After dialysis the ^{15}N wt solution was supplemented with 200 µM GTP, 20 µM taxol and 1 mM DTT. HSCQ was performed for 40 min at 5 °C with ^{15}N wt as reference. Protein concentrations of 400 µM were used in all measurements, if not specified otherwise. A tubulin fraction (see 2.3.2 Tubulin) was thawed and incubated with 200 µM GTP at 37 °C for 5 min. 20 µM taxol was added and the polymerization performed at 37 °C for 20 min. Another NMR sepctroscopy was done for 40 min at 5 °C with ^{15}N wt and 3.2 mg/ml microtubules. The tubulin polymerization was monitored by electron microscopy before polymerization, after polymerization and at the end of the HSQC measurements.

For competition, the dialysed ^{14}N wt was treated like the ^{15}N wt before. Final concentrations of 50 µM or 120 µM ^{14}N wt were added to a sample with microtubule and ^{15}N wt with concentrations of 3.3 mg/ml and 75 µM, respectively. As a control the same procedure was done with an equal volume of buffer instead of ^{14}N wt solution. Both measurements were done for 40 min at 5 °C.

2.4.2 HSQC ^{15}N wt with unpolymerized tubulin

Two different protocols were carried out. In a first approach the dialysed ^{15}N wt and a tubulin fraction were supplemented with 200 mM GTP and kept at 5 °C (no polymerization was done). An HSQC was performed for 40 min at 5 °C with ^{15}N wt (as reference) followed by a 2nd measurement with ^{15}N wt and 3.2 mg/ml tubulin. Protein concentrations of 400 µM were used in all measurements. Tubulin polymerization was monitored by electron microscopy. In the second approach neither taxol nor GTP were added to ^{15}N wt or the tubulin fraction to prevent tubulin polymerization. HSQC was performed for 40 min at 5 °C on with ^{15}N wt and 3.2 mg/ml tubulin. The tubulin polymerization status was analysed via electron microscopy.

2.4.3 PRE of MTSL-tagged ^{15}N mutants

For the PRE measurements each of the expressed 4 mutant proteins (2.1 Cloning) was individually tagged with MTSL before it was dialysed. The purified protein extract was thawed and 1 mM of DTT was added (to reduce disulfide bonds). Incubation was done for 15 min at room temperature. A PD-10 desalting column (GE Healthcare) was prepared and the reduced sample applied according to the manufacturer's protocol. After elution with reaction buffer the free thiol concentration was measured with DTNB. MTSL was added in 5 fold excess and incubation was done for 4-5 h at room temperature with gentle agitation. DTNB was used to follow the tagging reaction. Buffer was changed to MT assembly buffer with centrifugal filter units (Amicon Ultra-15 centrifugal filter units, 10,000 NMWL). The PRE measurements were done for 40 min at 5 °C with MTSL-tagged mutant proteins. Protein concentrations of 400 µM were used in all measurements. As reference the tagged proteins were treated with DTT (15 min at room temperature) or ascorbic acid (1 h at 37 °C) and measured again.

2.4.4 PRE of MTSL-tagged ^{15}N mutants with microtubules

Mutants were tagged with MTSL as described above and dialysed in MT assembly buffer. 200 µM GTP and 20 µM taxol were added to the sample solution containing 100 µM of MTSL-tagged protein, and a PRE experiment was performed for 40 min at 5 °C. A tubulin fraction was thawed and incubated with 200 µM GTP at 37 °C for 5 min. 20 µM taxol was added and polymerization was done at 37 °C for 20 min. A PRE measurement was done as before with concentrations of 100 µM MTSL-tagged ^{15}N mutant and 3.2 mg/ml microtubules. As reference the samples were treated with DTT (15 min at room temperature) or ascorbic acid (1 h at 37 °C) and measured again.

2.4.5 PRE of MTSL-tagged ^{15}N mutants with unpolymerized tubulin

Mutants were tagged with MTSL as described above and dialysed in MT assembly buffer. A PRE experiment was performed with a sample containing 100 µM of MTSL-tagged protein for 40 min at 5 °C. A tubulin fraction was thawed and kept at 5 °C (neither GTP nor taxol added).

A PRE measurement was done as described above with a sample containing 100 µM MTSL-tagged ^{15}N mutant protein and 3.2 mg/ml tubulin. As reference the samples were treated with DTT (15 min at room temperature) or ascorbic acid (1 h at 37 °C) and measured again.

2.4.6 Intermolecular PRE of MTSL-tagged ^{14}N A48C and ^{15}N wt

The A48C ^{14}N mutant was tagged with MTSL as described above and dialysed in MT assembly buffer. The ^{15}N wt was dialysed in the same buffer. For measurements with microtubule both samples were supplemented with 200 µM GTP and 20 µM taxol. PRE measurements were done with wt protein at concentrations of 75 µM for 40 min at 5 °C. Another PRE experiment was done at the same conditions with ^{15}N wt protein and ^{14}N A48C mutant protein, both at concentrations of 75 µM. For intermolecular measurements with microtubules a tubulin fraction was thawed and incubated with 200 µM GTP at 37 °C for 5 min. 20 µM taxol was added and polymerization was done at 37 °C for 20 min. A PRE measurement was done with a sample containing 75 µM ^{15}N wt protein and 3.2 mg/ml microtubules. 75 µM A48C ^{14}N was added and the solution measured again. For intermolecular measurements with tubulin a tubulin fraction was thawed and kept at 5 °C (neither GTP nor taxol added). A PRE measurement was done with a sample containing 75 µM of ^{15}N wt protein and 3.2 mg/ml microtubules. 75 µM A48C ^{14}N was added and the solution measured again.

PD-10 desalting column

The PD-10 desalting columns (GE Healthcare) are gel filtration columns packed with Sephadex G-25 medium. For details to gel filtration see 2.3.1 Gel filtration/Size exclusion chromatography.

DTNB

5,5'-dithiobis-(2-nitrobenzoic acid) (DTNB) or Ellman's reagent is a reagent to test for free thiols. The reagent reacts equimolar with thiols and forms NTB^-(2-nitro-5-thiobenzoate) which ionizes to NTB^{2-} in neutral and alkaline solutions. The result is a yellow coloured complex with an absorbance maximum at 412 nm. There are several extinction coefficients described

in the literature for different solution properties (high salt, dilute buffer solutions) that can be used in Lambert Beer's law to calculate the concentration of NTB^{2-} (hence free thiols). The concentration of thiols furthermore corresponds directly to the concentration of protein by a factor given by the amount of cysteines in one molecule.

3 Results

To investigate the overall structure of LC1-MTB NMR PRE experiments were done. Since a cysteine is necessary for PRE, we used the wt LC1-MTB clones from the backbone assignment (http://www.bmrb.wisc.edu/data_library/summary/index.php?bmrbId=18895) [44] and constructed 4 variants:

A26C aspartic acid 26 (position 2 excluding His-tag and linker) to cysteine

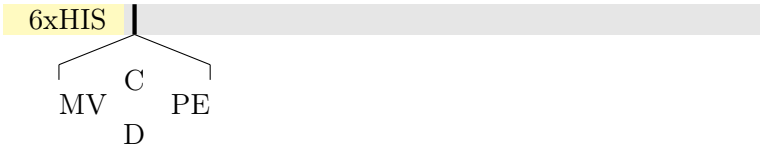

A48C alanin 48 (position 24 excluding His-tag and linker) to cysteine

S100C serine 100 (position 76 excluding His-tag and linker) to cysteine

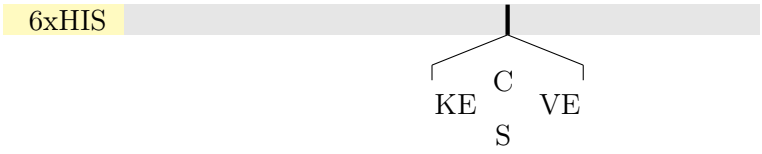

S136C serine 136 (position 112 excluding His-tag and linker) to cysteine

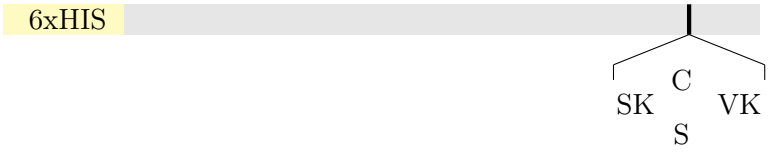

To learn more about the mechanism by which LC1-MTB binds to microtubules a set of HSQC and PRE experiments were done with wt and the mutant proteins.

Wt binding including competition

The ^{15}N wt was measured in the presence of polymerized microtubules or unpolymerized

tubulin to look for structural changes upon microtubule binding. Additionally, an unlabelled ^{14}N wt was used to assess if competition takes place and supports the previous binding data.

Mutant binding

The ^{15}N mutants were measured in absence and presence of microtubules or tubulin to check if PRE effects change after microtubule binding and reveal rearrangements of the overall structure (regions closing in on each other or getting further apart).

Intermolecular PRE

The ^{15}N wt was measured in the presence of polymerized microtubules and ^{14}N mutant A48C with spin label to get information about the distance between molecules bound to microtubules.

The wt and mutant proteins were expressed in *E. coli* BL21 Codon Plus (DE3) in the presence of ^{15}N ammonium chloride and purified by affinity (HisTrap FF Crude, GE Healthcare) and size exclusion (HiLoad 16/600 Superdex 200, GE Healthcare) fast protein liquid chromatography. Afterwards they were tagged with a spin label (MTSL), dialysed in 100 mM Pipes (1 mM EGTA, 1 mM $MgSO_4$, pH 6.8) and measured with NMR. MTSL-tagging was omitted for wt preparations (the NH_2-terminal domain of LC1 contains no cysteins), and the ^{14}N samples were grown with regular nitrogen sources.

3.1 HSQC measurements of ^{15}N wt

The HSQC measurements are standard 2-dimensional NMR experiments, giving information of two different atoms at once. Instead of a graph with intensities against chemical shifts (Δppm), the data is displayed as a contour plot. In that case, the chemical shifts of one atom (^{15}N) are plotted against the chemical shifts of the second atom (^{1}H). Additionally, it is often beneficial to blot signal intensities against amino acid residues.

3.1.1 ^{15}N wt with microtubules or tubulin

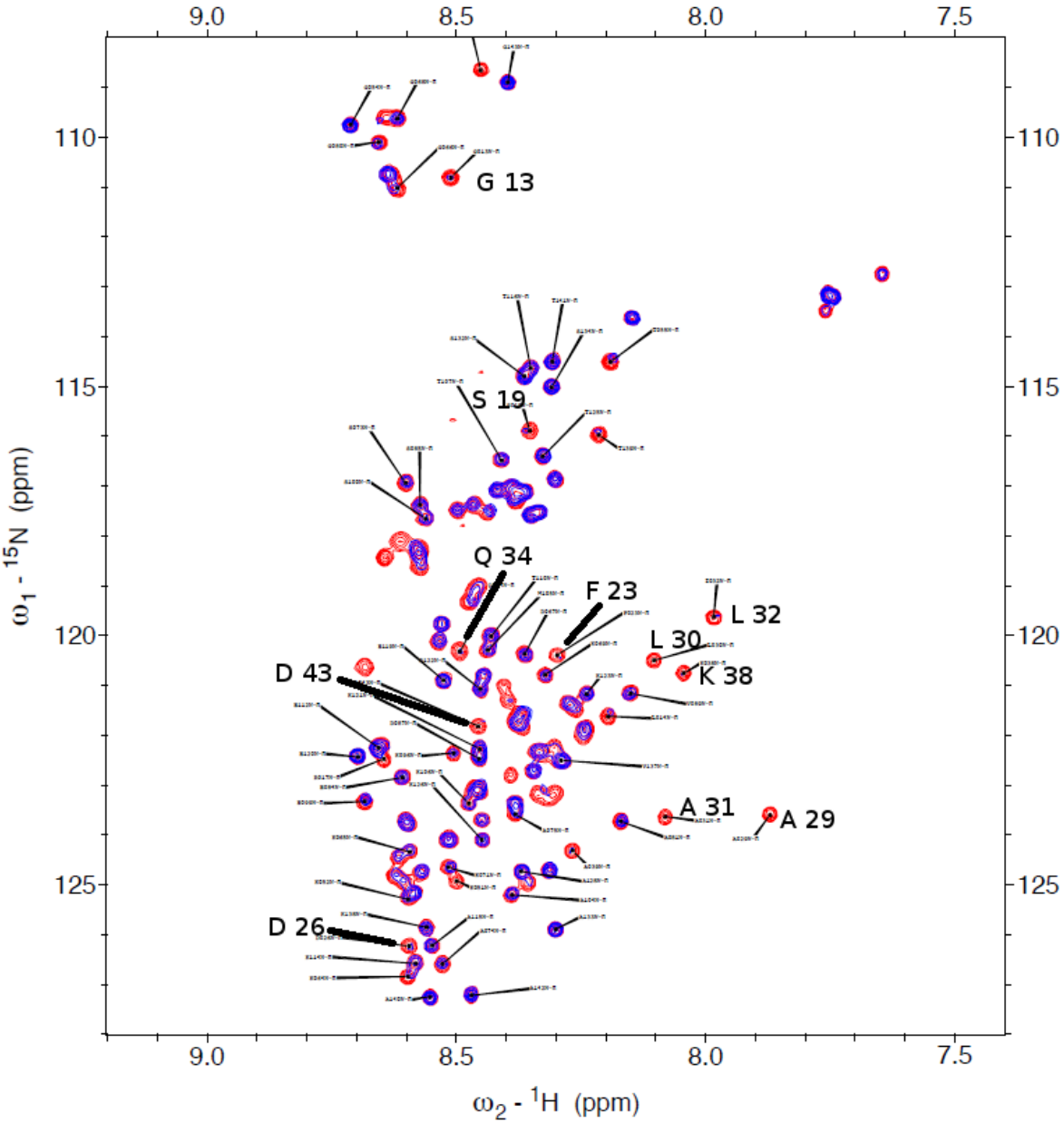

Figure 17: ^{15}N-HSQC spectrum of wt and wt with microtubules - Chemical shifts of ^{15}N nuclei are plotted against chemical shifts of ^{1}H nuclei. The red contours show ^{15}N wt in buffer only, while the blue contours correspond to ^{15}N wt in presence of microtubules. Many of the NH_2-terminal residues showed a decrease in signal intensity when microtubules were added, indicating that those residues were bound to the filaments.

Figure 17 shows the ^{15}N-HSQC spectrum of wt with and without microtubules. In presence of microtubules many of the N-terminal residues showed a decrease in signal intensity, indicating that they were bound to the rigid microtubules and could, as part of the complex, no longer be observed. This is because atoms in high molecular weight protein complexes have very short relaxation times, while, at the same time, steps with long delays (like the evolution period) are necessary for 2D-NMR. Thus, signals of large proteins complexes and molecules bound to them disappear between the different NMR steps (see 1.5.1 HSQC).

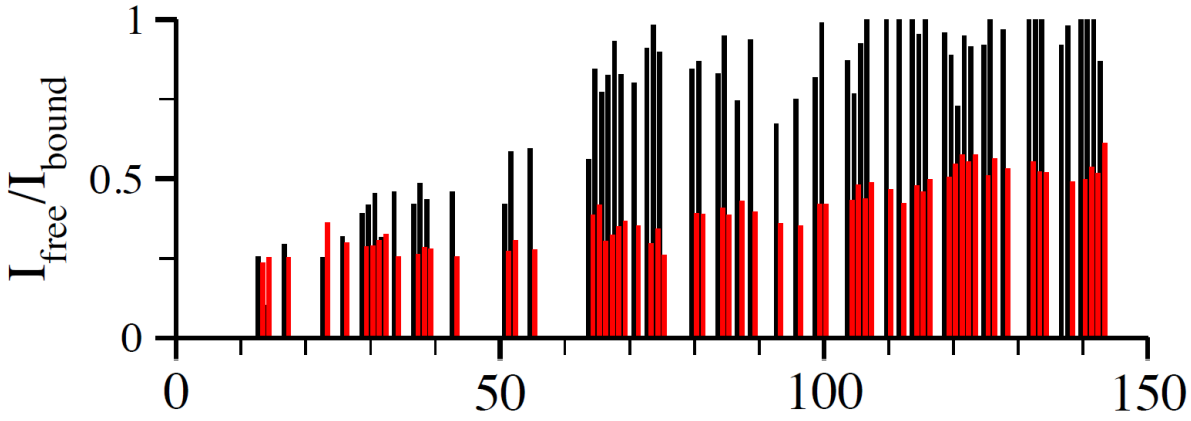

Figure 18: ^{15}N wt LC1-MTB bound to tubulin or microtubules - Signal intensities of bound residues are referenced to the intensities of their free form and plotted against the specific backbone position. The black colour corresponds to protein in presence of unpolymerized tubulin while red shows them in presence of microtubules. Both, measurements in presence of microtubule and tubulin, show signal loss in relation to free wt. While interaction with tubulin seems to require only the NH_2 terminus, microtubule binding appears to involve the whole protein.

In both experimental setups (wt with tubulin and wt with microtubules) an interaction between wt and microtubules or tubulin could be observed (Figure 18). Binding of wt to microtubules appeared to involve all residues although not equally strong. For the NH_2-terminal part (residues 25 to 60) of the protein the highest signal loss could be observed, thus the strongest binding can be inferred. The second, middle part (residues 61 to 100) seems to be slightly more mobile but still showed a high amount of signal loss. This could be due to intramolecular constraints of the molecule, restricting the movement of the middle part while the NH_2 terminus is bound. However, it is more likely due to moderately strong binding of the middle part to microtubules. The third, COOH-terminal part (residues 101 to 145) displayed even less involvement in the interaction, since the signal intensities were weakened the least. It may bind

to microtubules nevertheless, but could be in a more dynamic state than the other regions, thus alternating between a binding and a free state. In contrast to the results obtained with microtubule, binding of LC1-MTB to tubulin heterodimers was only detected for the NH_2-terminal region. Furthermore, it didn't seem to have significant limitations in mobility for the rest of the protein. This supports the idea of 3 binding regions with differently strong affinities for microtubules.

3.1.2 ^{14}N wt competition with microtubules

To determine whether the decrease in signal intensity of ^{15}N wt amino acid residues observed in the presence of microtubules is indeed due to their interaction with microtubules, we introduced competition. The ^{15}N wt and microtubule measurement was repeated in the presence of ^{14}N wt. Since ^{14}N has a quadrupole-moment, amino acids incorporating ^{14}N instead of ^{15}N show no signal in NMR spectroscopy. However, the ^{14}N wt protein is in most other aspects identical to ^{15}N wt. Hence, for each ^{14}N molecule binding to microtubules, a ^{15}N molecule should be released, thus leading to a gain in signal strength. Figure 19 shows the signal strength after addition of 50 µM and 120 µM ^{14}N wt to 75 µM ^{15}N wt. In both cases a gain of signal is obvious while intensities of protein without microtubules or tubulin are not reached. This supports the binding data shown before (see figure 18).

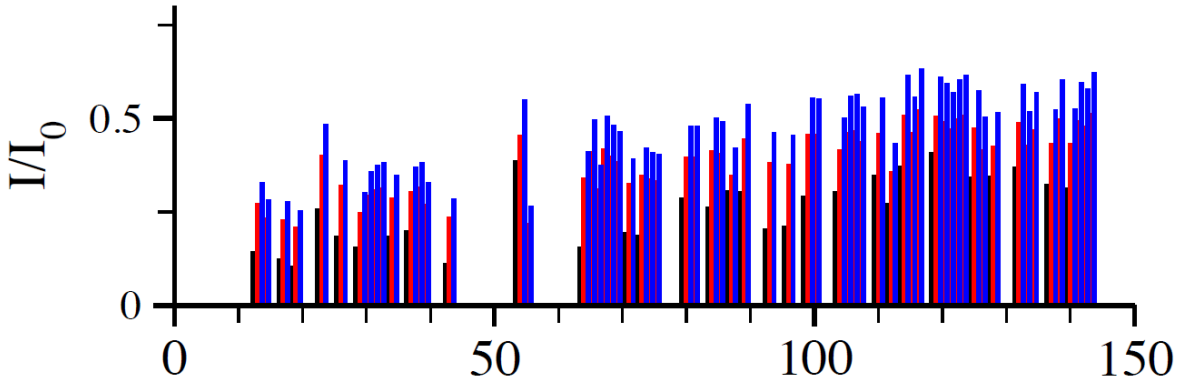

Figure 19: Intensity gain upon ^{14}N wt competition - The signal intensities are plotted against amino acid positions. Measurement of ^{15}N wt (75 µM) and microtubules (in black) shows no difference to earlier results. Upon addition of 50 µM ^{14}N wt (red) the signals increase in intensity, suggesting displacement of ^{15}N wt from microtubules. Addition of 120 µM ^{14}N protein (blue) leads to an even higher restoration of signal intensities.

3.2 PRE measurements of MTSL-tagged ^{15}N mutants

In PRE measurements the additional information compared to standard HSQC lies in potential differences of signal intensities of each amino acid. The paramagnetic group attached to an amino acid reduces the signal strength of neighbouring atoms, thus their signals intensities decrease. This decrease corresponds to the distance between the effected nucleus and the paramagnetic label. The effect of the paramagnetic label reaches about 20 Å, hence the signal intensity won't change significantly for atomic nuclei further away. The intensities provided by PRE give however no information about the original, unaltered intensities of the sample. For this purpose the results are generally provided as a ratio between the intensities with relaxation enhancement and the intensities without relaxation enhancement.

Keeping in mind the approximate distance of about 3.5 Å between successive amino acids in unfolded polypeptides, a decrease in signal intensities is expected for at least 5-6 amino acids flanking the label in both directions. Thus, the success of the tagging can be judged by a dent in signal strength of residues flanking the tagging position. Reduction in signal strength beyond or outside of this area may offer valuable support for hypothetical or predicted structure elements. For example, the distance between amino acids in α-helices with around 1.5 Å is much smaller than in unstructured regions. Moreover, a tangle of loops and turns can have a similar effect or may show PRE effects of even wider stretches. In general, signal intensity reductions that are not continuous with the area around the tagged residue or those stretching over a wide area provide evidence for contacts (i.e. distances of less than 20 Å) between the spin label and the affected residue.

3.2.1 MTSL-tagged D26C

The NMR PRE measurement of the MTSL-tagged ^{15}N D26C (see figure 20) showed a dent in signal intensities around position 26 (D1) stretching several amino acids to residue 31, suggesting a rather unfolded state in this region. Additionally there seems to be a small dent from residue 35 to 55 (D2), indicating a mean distance to the labelled residue, since the loss of signal intensities is not very pronounced. There is an area not affected by PRE, between the two dents (D1 and D2), thus there could be a turn between D1 and D2, just out of range

of the spin label. The intensity decrease from the label to the NH_2 terminus is not relevant, because this area is not part of the protein but part of the His-tag and linker sequence.

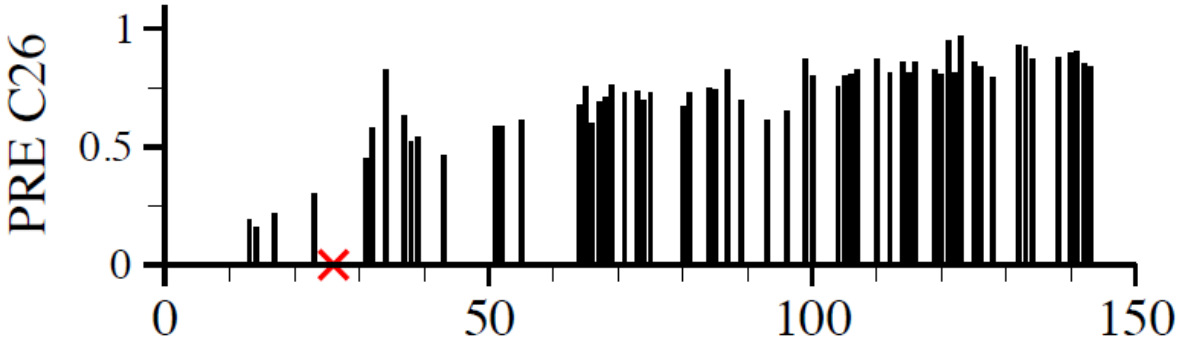

Figure 20: PRE measurement of MTSL-tagged ^{15}N D26C - The intensities show the ratio of the protein with the paramagnetic tag against the same protein with the tag quenched through ascorbic acid. These signal intensities are plotted against the backbone position. As expected, the near proximity of the MTSL-tag (at cysteine 26, marked with the red cross) shows a high amount of signal loss and stretches immediately for about 5 amino acids in direction of the COOH terminus. Signal loss in direction of the NH_2 terminus is not relevant, since this area contains the 6xHIS-tag. There is however a second small dent in signal intensities of residues 35 to 55.

3.2.2 MTSL-tagged A48C

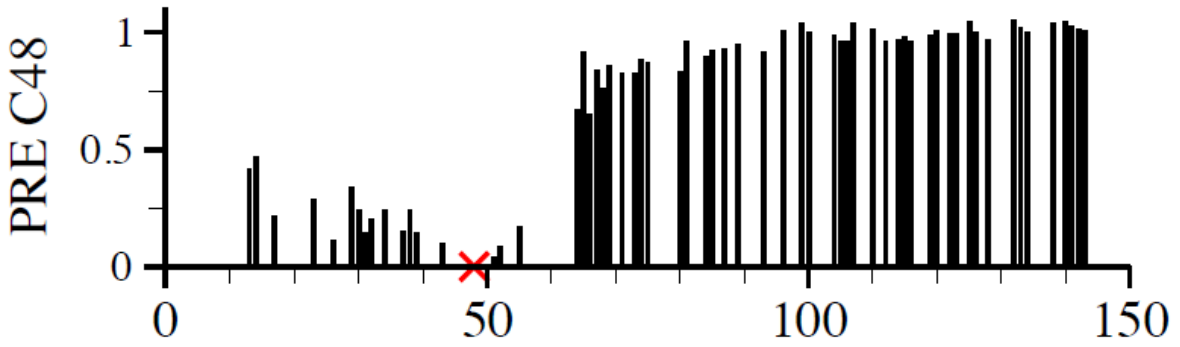

Figure 21: PRE measurement of MTSL-tagged ^{15}N A48C - The signal intensity of A48C with MTSL is referenced to A48C with the spin label quenched and plotted against the residue numbers. The effect of the paramagnetic label at position A48 (red cross) stretches far to lysine 64. Additionally, the region from the label to the N terminus seems to be affected even further.

Measurements of A48C (see figure 21) showed relaxation enhancement around position 48 (red cross) stretching far in both directions. Residues 25 through 65 seemed to be affected

by PRE and showed a decrease in signal intensities. This suggests dwelling of 23 (in NH_2-terminal direction) respectively 18 residues (in COOH-terminal direction) in near proximity of the paramagnetic label. An effect spanning only 5-6 amino acids in each direction would be expected for an entirely unfolded region, hence the broad dent in signal intensities implicates some kind of compaction of the residues around alanine 48.

3.2.3 MTSL-tagged S100C

The relaxation enhancement on S100C (see figure 22) showed a region of signal loss continuous with the label over a wide area. This suggests some clustering around serine 100 bringing many neighbouring residues closer to the label. However, there was no indication for another significant dent in signal intensities, suggesting that this region is not near any other part of the protein. This could be due to high density of clustering of the region around the label.

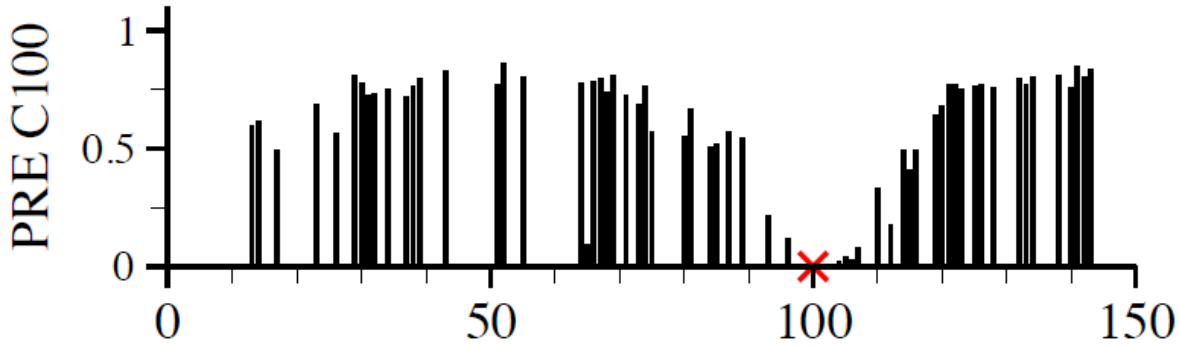

Figure 22: PRE measurement of MTSL-tagged ^{15}N S100C - The signal intensities are plotted against the amino acid positions. Intensities are referenced to S100C with the spin label quenched. The MTSL-label at position 100 (red cross) shows equal relaxation enhancement in both directions. The clearly visible dent shows that the further away a residue is from the tag, the weaker the signal loss.

3.2.4 MTSL-tagged S136C

The dent in signal intensities at the tagged cystein 136 (see figure 23) showed signal loss in near proximity to the paramagnetic group and thus suggests successful labelling. There was, however, similar to mutant S100C no other significant relaxation enhancement visible. Hence, the region around cystein 136 may never get close to other regions. It is also possible

for encounters to be so rare, that they don't have an impact on the average signal intensity obtained by NMR.

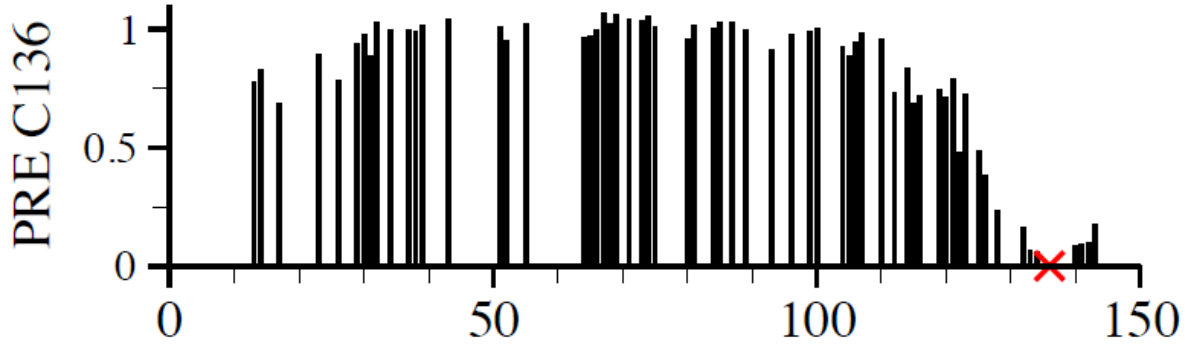

Figure 23: PRE measurement of MTSL-tagged ^{15}N S136C - The signal intensities are plotted vs. residue positions. Intensities of 136C with MTSL are referenced to S136C with MTSL quenched. The clearly visible relaxation enhancement around position 136 (red cross) indicates that the tagging worked fine. There is, however, no other significant signal loss in other regions of the protein.

3.3 MTSL-tagged ^{15}N mutants with microtubules or tubulin

Earlier data (3.1.1 ^{15}N wt with microtubules or tubulin) already showed that most of the amino acids of LC1-MTB are involved in microtubule binding. This raised the question how the overall structure of the protein may change as a consequence of this interaction. To asses this, mutants with spin labels were measured while interacting with microtubules or tubulin, to see if signal loss originates not only from binding to microtubules or tubulin, but also from near proximity to the spin label. Therefore the MTSL-tagged mutants were measured with microtubules or tubulin and without microtubules or tubulin, respectively. Furthermore, each of these measurements was repeated after quenching the spin label with ascorbic acid. The intensities from measurements with MTSL-tag were than referenced to their corresponding measurement with the tag quenched.

3.3.1 MTSL-tagged D26C with microtubules

The D26C mutant was measured with and without microtubules. The intensities of bound and free D26C were then compared to each other (see figure 24). Surprisingly, although the effect of PRE could be observed around residue 26 in both measurements, there was no evidence of

microtubule binding. It is possible that the mutation (D to C) at residue 26 is interfering with the binding of D26C to microtubules. However, more likely the MTSL-label attached to this residue introduces some clashes, thereby inhibiting effective binding to microtubules.

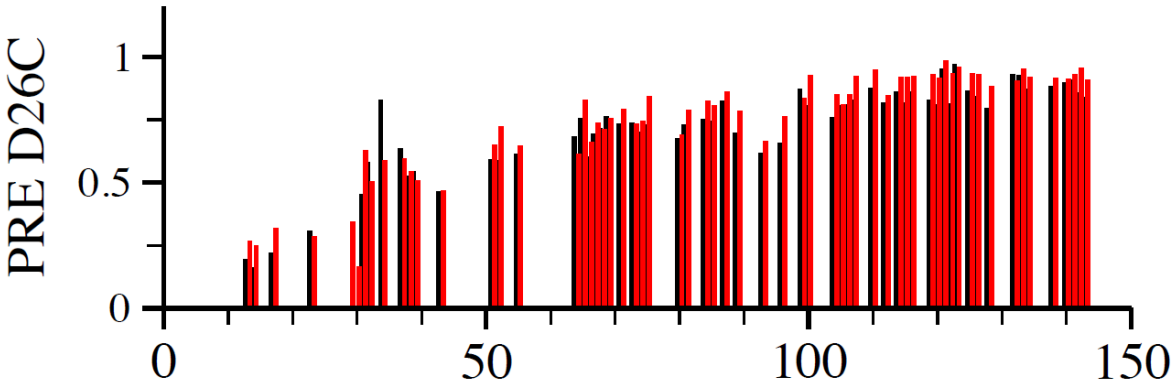

Figure 24: PRE measurement of MTSL-tagged^{15}N D26C with microtubules - Intensities of MTSL-tagged D26C mutant with microtubules (red) and without microtubules (black) are plotted against residue positions for comparison. The signal loss due to the paramagnetic group is clearly visible around residue 26 in both cases. Surprisingly, there is no signal reduction as we would have expected upon binding of D26C to microtubules.

3.3.2 MTSL-tagged A48C with microtubules or tubulin

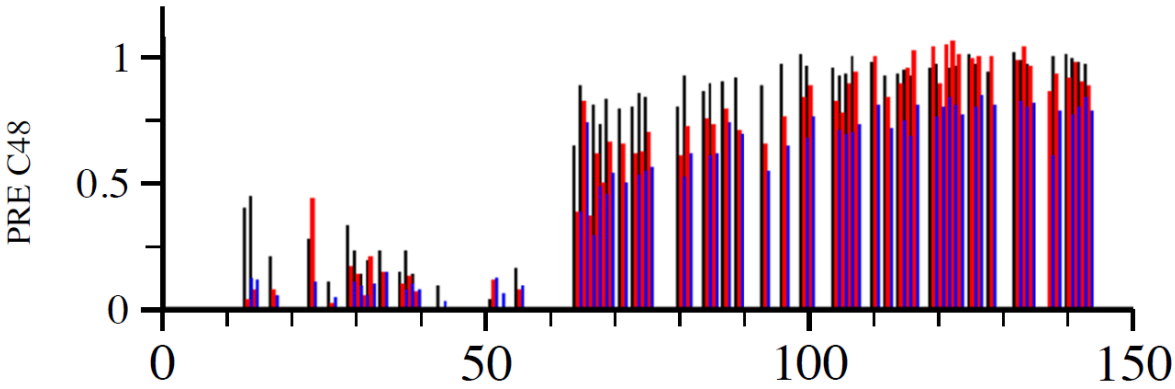

Figure 25: PRE measurement of MTSL-tagged ^{15}N A48C with microtubules or tubulin - Signal intensities are plotted against amino acid positions. There is already a high amount of signal loss through the paramagnetic relaxation enhancement at residue 48 without microtubules (black bars) that obscures the signal loss due to interaction with microtubules. However, some signal loss originating from binding to microtubules (blue) or tubulin (red) is still visible in the middle and COOH terminal parts of the protein.

The high amount of relaxation enhancement around residue 48 (see figure 25) mostly obscured the signal loss originating from binding to microtubules at the NH_2 terminus. However, the interaction with microtubules is still observable as a reduction in the middle and the COOH terminal parts of A48C. This is consistent with earlier findings in wt measurements (see figure 18). Surprisingly, tubulin binding did appear to show signal reduction in the middle part of LC1-MTB. Binding to tubulin without the spin label did not show the involvement of the middle part (see figure 18). Furthermore, the MTSL-tagged mutant without tubulin did not show any relaxation enhancement in this region as well (see figure 21). This means that the signal reduction appears only when the NH_2-terminal part of LC1-MTB is bound to tubulin and the residue 48 is MTSL-tagged. This suggest that upon binding to tubulin the middle part of LC1-MTB gets closer to residue 48 in its NH_2-terminal domain. The same might be true for microtubules, although we can not see the PRE effect because binding to microtubule involves the middle part of LC1-MTB and thus leads already to signal loss in this region. Hence, relaxation enhancement from the MTSL-label may be obscured by the interaction with microtubules.

3.3.3 MTSL-tagged S100C with tubulin

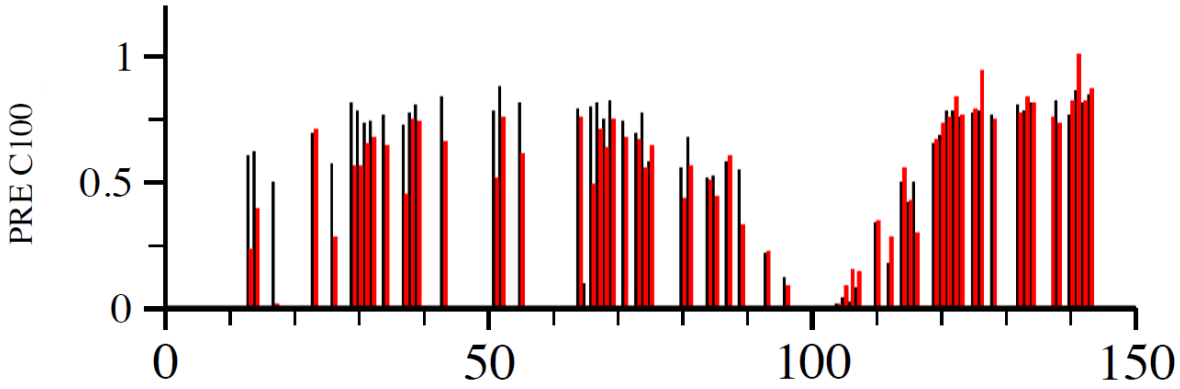

Figure 26: PRE measurement of MTSL-tagged ^{15}N S100C with tubulin - Signal intensities are plotted against residue positions. Tubulin binding (red) in mutant S100C seems to be weak, but is still observable. The signal intensities show enhanced relaxation around residue 100 as expected, but there is no other region visibly affected by the spin label, not even in the presence of tubulin.

The S100C mutant was not measured in presence of microtubules, but only in presence of unpolymerized tubulin (see figure 26). Comparison between the free protein and the protein in

the presence of tubulin showed only weak interaction in the NH_2-terminal region. This could be caused by a low concentration of functional tubulins in solution or by effects of the spin label. However, it is unlikely that the spin label is weakening the interaction with microtubule, since earlier results indicate that the NH_2 terminal region is the main part involved in interactions with microtubules. The PRE effect was clearly visible around residue 100, but there was no evidence for conformational change in response to tubulin binding causing a translocation of serine 100 to the near proximity of other regions.

3.3.4 MTSL-tagged S136C with microtubules or tubulin

Unfortunately the expression of S136C for measurement with microtubules or tubulin couldn't be done in time.

3.4 Intermolecular PRE with microtubules or tubulin

To assess if individual LC1-MTBs bind close to each other on microtubules, intermolecular PRE measurements were done. For this purpose ^{15}N wt was measured in presence of microtubules or tubulin. Furthermore, ^{14}N A48C was expressed and tagged with MTSL.^{14}N has a quadrupole-moment, thus the ^{14}N A48C molecule remains undetected in 2d-NMR. This means, no signal loss due to intramolecular PRE can be observed from the A48C mutant if it is added to the ^{15}N wt measurement. However, if the spin label on ^{14} N A48C comes into close proximity to the ^{15}N wt, relaxation enhancement can occur intermolecularly. Thus, dents in signal intensity of ^{15}N wt residues as a result of addition of ^{14} A48C indicate binding of LC1-MTB molecules next to each other on microtubules or tubulin heterodimers. Each measurement of ^{15}N wt with ^{14}N A48C and microtubules or tubulin was referenced to a corresponding measurement of ^{15}N wt without ^{14}N A48C and with microtubules or tubulin, respectively. Hence, signal loss originating from binding to microtubules or tubulin should be removed from the signal intensities.

As control a measurement was done with MTSL-tagged ^{14}N A48C and ^{15}N wt in solution. No intermolecular PRE could be observed (see figure 27), thus PRE by oligomerization of LC1-MTB could be ruled out.

Measurement with microtubules showed relaxation enhancement throughout the whole wt protein. This suggests that different LC1-MTB molecules bind next to each other on microtubules. The highest signal loss seems to be at the NH_2-terminal region, while the COOH terminus shows the least relaxation enhancement. Moreover, the signal loss due to intermolecular PRE follows a similar pattern as signal loss due to microtubule binding. This is reasonable, since parts that are bound strongly to microtubules are more often close to each other than parts that are less attached to microtubules and hence more mobile. Thus, the COOH terminus is more likely to be out of the effective PRE range than the NH_2 terminus. Measurement with tubulins showed that more than one LC1-MTB molecule is able to bind to tubulin-heterodimers. The signal reduction seems limited to the NH_2 terminus, similar to signal reduction upon binding to tubulin. This is again supported by previous binding data, showing LC1-MTB interaction with tubulins mainly through the NH_2-terminal residues (see figure 18), since residues not involved in binding to tubulin are more likely to be out of range of the MTSL-label on the neighbouring molecule.

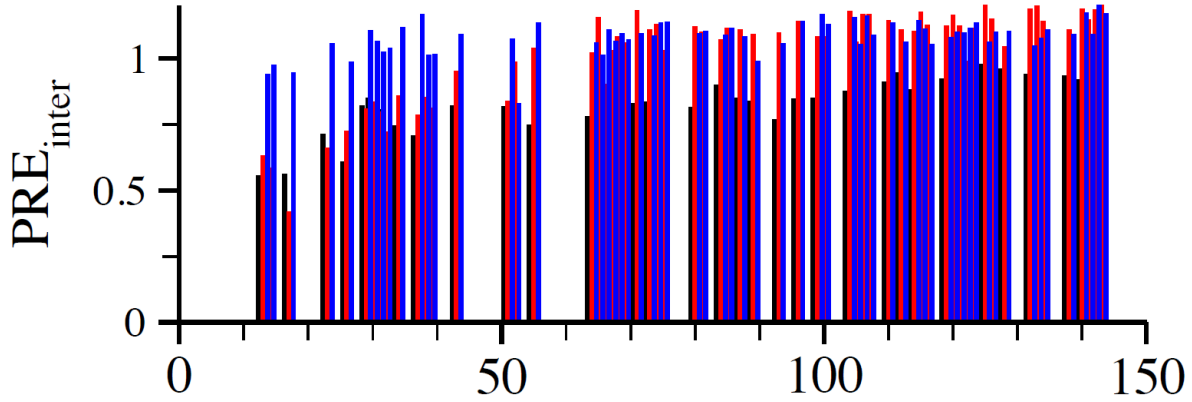

Figure 27: Intermolecular PRE measurement of MTSL-tagged ^{15}N wt and ^{14}N A48C with microtubules or tubulin - Intensities are plotted against residue positions. The measurement of ^{14}N A48C and ^{15}N wt in solution without microtubules (blue) shows no PRE. In contrast, a signal loss is recognizable when microtubules are added (black). Even if only unpolymerized tubulin is added, enhanced relaxation can be observed near the NH_2 terminus (red).

4 Discussion

4.1 NH_2- and COOH-terminal regions stay mostly separated in free molecules

In our PRE measurements of mutants without microtubules or tubulin some information about the major state of LC1-MTB could be gained. The COOH-terminal regions around serine 100 and serine 136 (see figures 22 and 23) did not show any proximity to each other or the rest of the protein. These regions may still come close in rare conformations that can not be detected by NMR (due to averaging), but seem to stay isolated in the more frequent conformations. The NH_2-terminal regions were shown to be more compact but did not show vicinity to regions of the COOH terminus. Our PRE results therefore provide no evidence for a majority in the assemble of structures that could bring NH_2- and COOH-terminal regions close to each other in solution, but support the idea of at least 2 mostly isolated regions of LC1-MTB.

4.2 The NH_2-terminal region could contain necessary structure elements for binding to microtubules

The MTSL-label attached to A48C suggested near proximity of this residue to the NH_2 terminal part of LC1-MTB (see figure 21). This observation was supported by PRE measurements of the protein labelled at position 26, although the effect in COOH-terminal direction was neither as continuous nor as strong as the effect from the label at residue 48 to the NH_2 terminus (see figure 20). Since the distance from 26 to 48 and from 48 to 26 has to be equal, we would have expected a similar result for PRE at 26C and 48C. Keeping in mind metastructure analysis and NMR secondary shifts, both showing a propensity to form an α-helix in this region, this could mean that either the mutation of asparagin to cystein at position 26, or the additional attachment of the MTSL-label interrupted folding and hence lengthened the distance between residues in this region. Support for this hypothesis comes from the PRE measurements with microtubules or tubulin. While both the 48C and 100C mutants interact with microtubules or tubulin, the results of the 26C mutant show no evidence for binding to microtubules (see figures 24-26). Unfortunately there was no time to complete the 136C mutant measurements, which would have given further clues. Hence, further investigation has to be done to clarify

if lack of interaction of 26C with microtubules is due to prevention of proper folding or other processes (for example steric clashes introduced by the MTSL-label).

4.3 Interaction with microtubules or tubulin showed 3 regions of different binding strength

Examining LC1-MTB by NMR revealed the residues involved in interactions with microtubules and tubulin. Binding to microtubules is likely to involve the whole LC1-MTB (see figure 18). Loss of signal intensity divides this part in 3 different regions. The first, NH_2-terminal part (residues 25 to 60) showed considerable loss in signal intensity and seems to be the major microtubule interaction domain. The middle part (residues 61 to 100) still had a high interaction potential, although this part may not be bound as stringent as the NH_2 terminus. The last, COOH-terminal part (residues 100 up to 145) showed the least interaction potential. This part may be alternating between a bound and free form during the period of interaction of LC1-MTB with microtubules. However, we have to keep in mind that in intact LC1 this COOH-terminal part of LC1-MTB is followed by the compact COOH-terminal domain of the full length LC1 and might merely act as a flexible linker between NH_2-terminal (microtubule binding) and COOH-terminal (actin and heavy chain binding) domains of intact LC1.

4.4 Involvement of the whole LC1-MTB may need protofilaments or lateral contacts

In contrast to microtubule binding, LC1-MTB interaction with unpolymerized tubulin seemed to be limited to the first, NH_2-terminal region. This suggests that this part is sufficient for binding to tubulin and could be sufficient for binding to microtubules as well. Support for this idea comes from LC1-MTB measurements with microtubules, showing the strongest interaction in the same NH_2-terminal region. The middle and COOH-terminal parts appear to be able to bind to microtubules but not tubulin heterodimers. A reason for this behaviour may be that NH_2-terminal, middle and COOH-terminal parts of LC1-MTB interact with different docking sites on tubulin heterodimers and microtubules. Polymerized microtubules consist of protofilaments arranged in parallel fashion. Thus, they contain 3 additional potential binding sites that are not present in tubulin heterodimers: the joint region between α- and β-tubulin along

the protofilament, the region of lateral contacts between tubulin heterodimers of neighbouring protofilaments and special lateral contacts at the seam (see 1.1.1 Microtubule structure). It is possible that one or more of these additional binding sites only present in microtubules are docking sites for the middle and/or COOH-terminal part of LC1-MTB, whereas its NH_2-terminal part interacts with surfaces on the microtubule that can also be found on the tubulin heterodimer.

4.5 Binding to tubulin may bring the middle part of LC1-MTB closer to its NH_2 terminus

When analysing tubulin binding of MTSL-tagged A48C (see figure 25) we observed a difference in signal strength in the middle part of LC1-MTB in comparison to measurements of free MTSL-tagged A48C and measurements of wt bound to tubulin. Analysis of free MTSL-tagged A48C and wt in the presence of tubulin showed no signal reduction in the middle part of the protein. In contrast the measurements of MTSL-tagged A48C and tubulin showed a slight reduction. This could mean that the middle part comes closer to the NH_2-terminal part upon tubulin binding. This may also happen in measurements with microtubule, but may not be visible since signals in the middle part are already reduced by binding to microtubules. Hence, relaxation enhancement caused by the spin label may be obscured.

4.6 More than one LC1-MTB is able to bind tubulin heterodimers

Intermolecular PRE revealed close proximity between LC1-MTBs when interacting with microtubules (see figure 27). Relaxation enhancement by binding of LC1-MTB molecules to one another could be ruled out by measuring them in absence of microtubules and tubulin. Measurements of ^{15}N wt, ^{14}N A48C with MTSL and microtubules showed a similar pattern of signal loss as ^{15}N wt microtubule binding. This suggests that the NH_2 terminus comes close to the NH_2 terminus of neighbouring molecules more often than the middle part and the COOH terminus and supports the idea that the NH_2 terminus is generally bound strongest to microtubules and tubulin. Furthermore, interaction with tubulin shows only relaxation enhancement in the NH_2 terminus. Since other parts do not interact with tubulin-heterodimers they may be simply

to far away from neighbouring molecules to be affected by relaxation enhancement. Additionally, PRE effects upon binding to tubulin showed that binding of more than one LC1-MTB per heterodimer is possible. This seems surprising since the heterodimer is the repetitive unit in microtubules and one might assume to see one LC1-MTB per heterodimer. However, there are many identical and similar residues — protein blast (http://blast.ncbi.nlm.nih.gov/Blast.cgi) showes 40 % identities and 60 % similarities — between α- and β-tubulin from porcine (*Sus scrofa*), from which several are located on the outer surface of tubulins and microtubules [48,49]. It is likely that there is a similar docking site for the NH_2-terminal region of LC1-MTB on both the α- and β-tubulin (similar to stathmin, see 1.2.3 Heterodimer binding proteins).

Our data does not allow to draw firm conclusions on how LC1-MTB molecules are arranged on microtubules. It is however likely that LC1-MTBs interact in a manner that allows all 3 regions (NH_2-terminal, middle and COOH-terminal parts) to get close to residues 48 on the neighbours NH_2 terminus, although the two later regions may keep more distance or may not remain in close proximity to residue 48 as long as the NH_2 terminus.

List of abbreviations

MAP	microtubule associated protein
LC1	light chain 1
LC1-MTB	light chain 1 microtubule binding domain
NMR	nuclear magnetic resonance
HSQC	heteronuclear single-quantum correlation
PRE	para-magnetic relaxation enhancement
FID	free induction decay
IDP	intrinsically disordered protein
ppm	parts per million
wt	wild-type
MTSL	1-oxyl-2,2,5,5-tetramethyl-3-pyrolin-3-yl)methyl methanthiosulfonate
GTP	guanosine triphosphate
+TIP	plus-end tracking protein
EB	end-binding protein
CH	calponin homology
MH1/2/3	MAP1 homology 1/2/3
FPLC	fast protein liquid chromatography
ddH_2O	double-distilled water
SDS	sodium dodecyl sulfate
DTT	dithiothreitol
BCA	bicinchoninic acid
PC	phosphocellulose
DTNB	5,5'-dithiobis-(2-nitrobenzoic acid), also Ellman's reagent
i.e.	id est (that is)
vs	versus

References

[1] Eckhard Mandelkow and Eva-Maria Mandelkow. Microtubules and microtubule-associated proteins. 7(1):72–81.

[2] Eckhard Mandelkow and Eva-Maria Mandelkow. Microtubule structure. 4(2):171 – 179.

[3] Cecilia Conde and Alfredo Cáceres. Microtubule assembly, organization and dynamics in axons and dendrites. 10(5):319–332.

[4] Sandrine Etienne-Manneville. Microtubules in cell migration. 29(1):471–499.

[5] Isabelle Arnal and Richard H. Wade. How does taxol stabilize microtubules? 5(8):900–908.

[6] R. Sato-Yoshitake, Y. Shiomura, H. Miyasaka, and N. Hirokawa. Microtubule-associated protein 1b: molecular structure, localization, and phosphorylation-dependent expression in developing neurons. 3(2):229–238.

[7] Julia R. Kardon and Ronald D. Vale. Regulators of the cytoplasmic dynein motor. 10(12):854–865.

[8] Claudia Veigel and Christoph F. Schmidt. Moving into the cell: single-molecule studies of molecular motors in complex environments. 12(3):163–176.

[9] Young-Hwa Song and Eckhard Mandelkow. Recombinant kinesin motor domain binds to beta-tubulin and decorates microtubules with a b surface lattice. 90(5):1671–1675.

[10] W. B. Redwine, R. Hernandez-Lopez, S. Zou, J. Huang, S. L. Reck-Peterson, and A. E. Leschziner. Structural basis for microtubule binding and release by dynein. 337(6101):1532–1536.

[11] Naoko Mizuno, Shiori Toba, Masaki Edamatsu, Junko Watai-Nishii, Nobutaka Hirokawa, Yoko Y. Toyoshima, and Masahide Kikkawa. Dynein and kinesin share an overlapping microtubule-binding site. 23(13):2459–2467.

[12] Günther Woehlke, Aaron K. Ruby, Cynthia L. Hart, Bernice Ly, Nora Hom-Booher, and Ronald D. Vale. Microtubule interaction site of the kinesin motor. 90(2):207–216.

[13] Melissa A. Gee, John E. Heuser, and Richard B. Vallee. An extended microtubule-binding structure within the dynein motor domain. 390(6660):636–639.

[14] C. O. De Groot, I. Jelesarov, F. F. Damberger, S. Bjelic, M. A. Scharer, N. S. Bhavesh, I. Grigoriev, R. M. Buey, K. Wuthrich, G. Capitani, A. Akhmanova, and M. O. Steinmetz. Molecular insights into mammalian end-binding protein heterodimerization. 285(8):5802–5814.

[15] Anna Akhmanova and Michel O. Steinmetz. Tracking the ends: a dynamic protein network controls the fate of microtubule tips. 9(4):309–322.

[16] Camelia Iancu Rubin and George F. Atweh. The role of stathmin in the regulation of the cell cycle. 93(2):242–250.

[17] Benoît Gigant, Patrick A. Curmi, Carole Martin-Barbey, Elodie Charbaut, Sylvie Lachkar, Luc Lebeau, Samila Siavoshian, André Sobel, and Marcel Knossow. The 4 Å x-ray structure of a tubulin:stathmin-like domain complex. 102(6):809 – 816.

[18] Shelley Halpain and Leif Dehmelt. The MAP1 family of microtubule-associated proteins. 7(6):224.

[19] Z. Orban-Nemeth. Microtubule-associated protein 1s, a short and ubiquitously expressed member of the microtubule-associated protein 1 family. 280(3):2257–2265.

[20] KarenA Butner and Marc W. Kirschner. Tau protein binds to microtubules through a flexible array of distributed weak sites. 115(3):717–730.

[21] A. Langkopf, J. A. Hammarback, R. Müller, R. B. Vallee, and C. C. Garner. Microtubule-associated proteins 1a and LC2. two proteins encoded in one messenger RNA. 267(23):16561–16566.

[22] Martin Tögel, René Eichinger, Gerhard Wiche, and Friedrich Propst. A 45 amino acid residue domain necessary and sufficient for proteolytic cleavage of the MAP1b polyprotein precursor. 451(1):15–18.

[23] Suzanne S. Mann and James A. Hammarback. Molecular characterization of light chain 3. a microtubule binding subunit of MAP1a and MAP1b. 269(15):11492–11497.

[24] Waltraud Kutschera, Wolfgang Zauner, Gerhard Wiche, and Friedrich Propst. The mouse and rat {MAP1B} genes: Genomic organization and alternative transcription. 49(3):430 – 436.

[25] Rainer Noiges, René Eichinger, Waltraud Kutschera, Irmgard Fischer, Zsuzsanna Németh, Gerhard Wiche, and Friedrich Propst. Microtubule-associated protein 1a (MAP1a) and MAP1b: light chains determine distinct functional properties. 22(6):2106–2114.

[26] Anibal Cravchik, David Reddy, and Andrew Matus. Identification of a novel microtubule-binding domain in microtubule-associated protein 1a (MAP1a). 107(3):661–672.

[27] W. Zauner, J. Kratz, J. Staunton, P. Feick, and G. Wiche. Identification of two distinct microtubule binding domains on recombinant rat MAP 1b. 57(1).

[28] Céline Bouquet, Michèle Ravaille-Veron, Friedrich Propst, and Fatiha Nothias. MAP1b coordinates microtubule and actin filament remodeling in adult mouse schwann cell tips and DRG neuron growth cones. 36(2):235–247.

[29] André Vandecandelaere, Barbara Pedrotti, Michelle A. Utton, Rosy A. Calvert, and Peter M. Bayley. Differences in the regulation of microtubule dynamics by microtubule-associated proteins MAP1b and MAP2. 35(2):134–146.

[30] N. Trivedi. Glycogen synthase kinase-3 phosphorylation of MAP1b at ser1260 and thr1265 is spatially restricted to growing axons. 118(5):993–1005.

[31] Robert G. Goold, Rebecca Owen, and Phillip R. Gordon-Weeks. Glycogen synthase kinase 3beta phosphorylation of microtubule-associated protein 1b regulates the stability of microtubules in growth cones. 112(19):3373–3384.

[32] Martin Tögel, Gerhard Wiche, and Friedrich Propst. Novel features of the light chain of microtubule-associated protein MAP1b: microtubule stabilization, self interaction, actin filament binding, and regulation by the heavy chain. 143(3):695–707.

[33] Heike Stroissnigg, Alžbeta Trančíková, Luise Descovich, Jakob Fuhrmann, Waltraud Kutschera, Julius Kostan, Arabella Meixner, Fatiha Nothias, and Friedrich Propst. S-nitrosylation of microtubule-associated protein 1b mediates nitric-oxide-induced axon retraction. 9(9):1035–1045.

[34] Phillip R. Gordon-Weeks and Itzhak Fischer. MAP1b expression and microtubule stability in growing and regenerating axons. 48(2):63–74.

[35] R. P. Tucker and A. I. Matus. Developmental regulation of two microtubule-associated proteins (MAP2 and MAP5) in the embryonic avian retina. 101(3):535–546.

[36] Arabella Meixner, Silke Haverkamp, Heinz Wässle, Susanne Führer, Johann Thalhammer, Nina Kropf, Reginald E. Bittner, Hans Lassmann, Gerhard Wiche, and Friedrich Propst. MAP1b is required for axon guidance and is involved in the development of the central and peripheral nervous system. 151(6):1169–1178.

[37] C. Bouquet. Microtubule-associated protein 1b controls directionality of growth cone migration and axonal branching in regeneration of adult dorsal root ganglia neurons. 24(32):7204–7213.

[38] C Gonzalezbillault. Perinatal lethality of microtubule-associated protein 1b-deficient mice expressing alternative isoforms of the protein at low levels. 16(4):408–421.

[39] P. Opal, J. J. Garcia, F. Propst, A. Matilla, H. T. Orr, and H. Y. Zoghbi. Mapmodulin/leucine-rich acidic nuclear protein binds the light chain of microtubule-associated protein 1b and modulates neuritogenesis. 278(36):34691–34699.

[40] Elizabeth Allen, Jianqing Ding, Wei Wang, Suneet Pramanik, Jonathan Chou, Vincent Yau, and Yanmin Yang. Gigaxonin-controlled degradation of MAP1b light chain is critical to neuronal survival. 438(7065):224–228.

[41] Yong Q. Zhang, Adina M. Bailey, Heinrich JG Matthies, Robert B. Renden, Mark A. Smith, Sean D. Speese, Gerald M. Rubin, and Kendal Broadie. Drosophila fragile x-related gene regulates the MAP1b homolog futsch to control synaptic structure and function. 107(5):591–603.

[42] Victoria Brown, Peng Jin, Stephanie Ceman, Jennifer C. Darnell, William T. O'Donnell, Scott A. Tenenbaum, Xiaokui Jin, Yue Feng, Keith D. Wilkinson, Jack D. Keene, and others. Microarray identification of FMRP-associated brain mRNAs and altered mRNA translational profiles in fragile x syndrome. 107(4):477–487.

[43] Jennifer C. Darnell, Kirk B. Jensen, Peng Jin, Victoria Brown, Stephen T. Warren, and Robert B. Darnell. Fragile x mental retardation protein targets g quartet mRNAs important for neuronal function. 107(4):489–499.

[44] Zsuzsanna Orbán-Németh, Morkos A. Henen, Leonhard Geist, Szymon Żerko, Saurabh Saxena, Jan Stanek, Wiktor Koźmiński, Friedrich Propst, and Robert Konrat. Backbone and partial side chain assignment of the microtubule binding domain of the MAP1b light chain. 8(1):123–127.

[45] Jörg Gsponer and M. Madan Babu. The rules of disorder or why disorder rules. 99(2):94–103.

[46] Peter Tompa. The interplay between structure and function in intrinsically unstructured proteins. 579(15):3346–3354.

[47] Robert Konrat. NMR contributions to structural dynamics studies of intrinsically disordered proteins. 241:74–85.

[48] J. Löwe, H. Li, K. H. Downing, and E. Nogales. Refined structure of ab-tubulin at 3.5 a resolution. 313(5):1045–1057.

[49] Eva Nogales, Michael Whittaker, Ronald A. Milligan, and Kenneth H. Downing. High-resolution model of the microtubule. 96(1):79–88.

Curriculum Vitae

Personal Information

Name:	Markus Huber
Citizenship:	Austria
Contact:	Markus.Huber@eclipso.at

Education

since 2012	Graduate studies in Molecular Biology (Cell Biology), University Vienna
2009 – 2012	Undergraduate studies in Biology (Molecular Biology), University Vienna
2001 – 2006	HTBLA Leonding, Austria majoring in computer science and organization

Employment

2007 – 2009	Software developer at 3BEG, Linz, Austria

Teaching Experience

03/2014 and 11/2014	Practice in Cell Biology, University Vienna
since 2013	Tutor at the Vienna Open Lab

Research Experience

since 07/2013	MSc Thesis "*Structural features of the MAP1b light chain 1 microtubule binding domain*", Group Propst in collaboration with Group Konrat, MFPL, Vienna *Methods: mutagenesis, protein expression (E. coli), FPLC (ÄKTA), SDS PAGE/western blot, spectrophotometry, tubulin preparation (porcine brain), protein tagging (MTSL)* Research on MAP1s KO mice *Methods: isolation of dermal fibroblasts (newborn and adult mice), immunofluorescence, live cell imaging*
10/2012 – 12/2012	Internship, Group Propst, MFPL, Vienna Structure determination of the N terminus of MAP1b light chain 1
07/2012 – 08/2012	BSc Thesis, Group Jantsch, MFPL, Vienna Different approaches for TALE construction

Scholarships

2013	Excellence Scholarship (Bundesministerium für Wirtschaft und Forschung)

Skills

Languages	German (mother tongue), English (very good)
Computer	Excellent knowledge of standard software: MS Windows, Linux (bash), MS Office, OpenOffice, Adobe Photoshop, GIMP, ImageJ, Latex, etc.
	Programming skills in C/C++/C#, Java, SQL/PLSQL, HTML, PHP and Phyton